The Hong Kong Polytechnic University

Department of Health Technology and Informatics

Poly(L-lactide)/Multiwalled Carbon Nanotube Composites: Mechanical Properties and Interaction with Osteoblast-like Cells in Vitro

By

POW Yu Fung

A thesis submitted in partial fulfilment of the requirements of

the degree of Master of Philosophy

December 2007

Certification of Originality

I hereby declare that this thesis is my own work and that, to the best of my knowledge and belief, I reproduce no material previously published or written, nor material that has been accepted for the award of any other degree or diploma, except where due acknowledgement has been made in the text

_____

Pow Yu Fung

Abstract

Tissue engineering is a potential solution for tissue reconstruction and function restoration. Scaffolds made by biocompatible biomaterial are important to provide guidance for cell growth and is required for tissue production. Therefore, the properties of biomaterial are important parameters to the success of tissue engineering. For bone tissue engineering, bone cell is sensitive to the mechanical environment and may be sensitive to changes of mechanical properties of scaffold. Poly (L-lactide) (PLLA) is a popular biomaterial with good mechanical properties. However, the weak mechanical property of PLLA scaffold hinders its wide application for bone tissue engineering. Reinforcing PLLA with other materials can be a good solution to address this problem. Multi-walled carbon nanotube (MWCNT), which is a novel nanomaterial with excellent mechanical properties, is a potential material for biomaterial reinforcement. However, the biocompatibility and bioactivity of this material is not clear. In this study, PLLA/MWCNT composite with different loading of MWCNT was applied for surface mechanical property reinforcement. Physical characterisation and biological study were carried out to evaluate its physical properties and biological interaction with human osteoblast-like cells (Saos2) (HOB).

Multi-walled carbon nanotubes (MWCNT) were dispersed by high power ultrasound. PLLA was dissolved in chloroform. PLLA/MWCNT composite with different ratio of PLLA to MWCNT was fabricated using solvent-casting techniques. The composite was characterized by SEM, EDX and XRD. From the SEM pictures, random distribution of dispersed MWCNT was observed from the composite surface. Some tubular MWCNT was protruded from the surface. EDX spectrum showed an increase in carbon content for PLLA/MWCNT composite with more MWCNT. MWCNT was detected by XRD and showed the successful incorporation of MWCNT

into PLLA. Nanoindentation was carried out and showed a higher in Young's modulus for sample reinforced with MWCNT.

The composite was coated with fibronectin to study the response of HOB cell. Fixed amount of cell was cultured on composite with different PLLA/MWCNT ratio. To monitor the morphology of the cell cultured on the composite, SEM pictures were taken and found that HOB cell was successfully adhered on the composite surface. They showed good cell morphology and did not have apparent morphological differences. The cytoskeleton of HOB cell was monitored by confocal scanning microscopy. Both composites showed stressed cytoskeleton fibre and good adhesion to the surface. The viability of cell was distinguished by trypan blue staining and cytometric counting. After 2, 4, 6 and 8 days culturing, the viability of cell was evaluated. It was found that cell cultured on different samples had over 90% viability on day 2, 4, 6 and 8. No significant differences of cell viability were found. It was expected that there is no significant cytotoxicity of PLLA/MWCNT composite over the biocompatible control sample. The activity of mitochondrial dehydrogenase (MD) enzyme and alkaline phosphatase (ALP) enzyme was evaluated by MTT substrate and p-nitrophenyl phosphate substrate. For the result of MTT assay, it was found that both PLLA/6.25% MWCNT and PLLA/5.00% MWCNT had significant differences from the control for all four different culture days. For ALP activity, it was found that sample with higher MWCNT content had generally higher ALP activity. However, no significant differences were found statistically. It seems that the incorporation of MWCNT into PLLA can increase the MD activity, but not the ALP activity significantly. It was found that sample with more MWCNT may still have certain advantages over the control.

Acknowledgement

I would like to express my gratitude to my supervisor, Dr Mo Yang, for his guidance, encouragement and support in this project.

I would like to thank my co-supervisor, Professor Arthur Mak and Dr Man Sau Wong for their advice and support.

I sincerely thank Dr Tony To, Dr Thomas Li, Ms Carina Luk, Mr Lui Ng, Ms Cherie Ko, Mr Ngork Wah Poon, Ms Vincy Wong, Dr John Yuen, Mr Terry Yu, Mr Adele Xiao, Mr Sammy Siu from Department of Health Technology and Informatics, for their advice and assistance. Ms Kam Lan Yeung and Ms Helen Mok from Department of Applied Biology and Chemical Technology for their assistance in confocal laser scanning microscopy and tissue culture. I thank Mr Jeremy Yeung from MRC for SEM, EDX and XRD service and training.

Finally, I would like to thank friends and colleagues of Department of Health Technology and Informatics

Last but not least, I have to thank my parent and sister for their support and caring throughout these two years.

Content

List of Figures

List of Tables

Acronyms

ALP	Alkaline phosphatase
cfPBS	Calcium-free phosphate-buffered saline
CNT	Carbon Nanotube
EDX	Energy dispersive X-ray spectrometry
FBS	Foetal bovine serum
HA	Hydroxyapatite
HOB	Osteoblast-like cell from human
MTT	3-[4,5-dimethyl-thiazol-2-yl]-2,5-diphenyltetrazolium bromide
MWCNT	Multi-walled carbon nanotube
PLLA	Poly (L-lactide)
SEM	Scanning electron microscopy
XRD	X-ray diffractometry

Chapter 1: Introduction

1.1. Motivation and Objective

Bone tissue is an important tissue in our body with numerous functions. However, in severe bone damages, bone tissue has relatively limited recovery power and may affect the quality of life of patient.

Several tradition solutions had been used to repair and restore the function of bone tissue. They are autogenic graft, allogenic graft, isogenic graft and xenogenic graft. However, they have some limitations such as limited supply and potential immunogenicity. Tissue engineering, which engineers the artificial tissue from the receiver, can be an alternative solution for repairing the bone tissue damages.

To engineer bone tissue, biomaterials and cell are two important factors which are required for tissue engineering. Biomaterial provides surface for cell adhesion, cell proliferation and cell differentiation. Cell is responsible for tissue deposit. Therefore, careful selection of biomaterials and cells for 3D scaffold fabrication is essential to the success of tissue engineering.

Poly (L-lactide) (PLLA) is a popular biomaterial because of its good mechanical properties and biocompatibility. A lot of study has been done to evaluate the possibility of scaffold fabrication and potential application in bone tissue engineering. Multi-walled carbon nanotubes (MWCNT) are a carbon-based nanomaterial and have received good attention because of its excellent mechanical and electrical properties. It has been studied for drug delivery and other biomedical application. It may be another attractive

material for tissue engineering when its biocompatibility and cytotoxicity have been thoroughly studied.

The objective of this research study is to evaluate the biocompatibility and mechanical properties of the PLLA/MWCNT composite and examine its potential application in bone tissue engineering. The study has been divided into several parts. The first part is the evaluation of possibility of fabricating PLLA/MWCNT composite by solvent casting technique. The second part is to assert the mechanical performance of PLLA before and after reinforced by MWCNT. Then the viability of osteoblast-like cell has been studies to estimate the cytotoxicity effect of MWCNT. Finally, the metabolic rate and bone matrix production marker have been studied to understand the cell response.

1.2. Scope and Outline of Thesis

This research project consists of two main parts

- Fabrication of PLLA/MWCNT composite.
- Cell seeding and evaluation of cell response.

This thesis is divided into six chapters. Chapter one consists of an overview of the thesis. Chapter two provides the information of the work done by the other scientist. It also includes general overview of bone tissue, different types of biomaterials, different method for scaffold fabrication and different important cell-specific response. Chapter three presents the detail procedures involved in PLLA/MWCNT composite fabrication, cell seeding and response characterization. Chapter four provides the result

of physical characterization of PLLA/MWNCT composite and biological result of seeding of osteoblast-like cell. Chapter five discusses the characterisation result of PLLA/MWNCT composite and seeding of osteoblast-like cell. Chapter 6 concludes the findings from this study and provides some future directions.

Chapter 2: Background

2.1. Bone, its repair and regeneration

2.1.1. Architecture of Bone Tissue

Tissue in our body is delicate and subject to damage easily. For slight injury, except a few types of tissue such as brain tissue, most tissues have their own recovery mechanism and can carry out self-repairing. However, in some serious cases, such as trauma, inflammation and tumours, reconstruction of tissue segments are required. By the own self-repairing capability of the tissue, the recovery period can be very long or even impossible. It may not allow complete function restoration. One of the good examples is the bone tissue (Martina et al., 2005).

Bone tissue can be divided into cortical bone and trabecular bone. Cortical bone can be found underneath the periosteum and is also known as lamellar bone. It is highly dense and comparatively acellular. It is mechanically stronger than trabecular bone. Trabecular bone is lying inside the cortical bone and is classified as woven bone. The cavities found inside trabecular bone is occupied by red or yellow bone marrow. It is more metabolically active than cortical bone.

Bone tissue also contains numerous mineralized proteins. Collagen and fibrous protein are the main components of all connective tissues. Collagen represents approximately 90% of the bone organic matrix. At least 20 different polypeptide chains are found which can form 16 different types of collagens. In bone tissue and other connective tissue, type 1 collagen shares the highest ratio in collagen family. However, they have different degree of cross-linking and different amount of glycosylation for

different function expression. Besides type 1 collagen, trace amount of types 3,5,12 and 13 collagen are detected in bone tissue. Collegan contains a contain cell attachment sequence and suggests their potential function for cell adhesion. It has no nucleation site for the deposition of hydroxyapatite. It is suggested that collagen may involve in binding and orientating other extracellular matrix protein. It is confirmed by the experiment carried out by Harber K et al (1984) that there is no bone formation in mouse if there is a mutation of polypeptide chain involved in type-1 collagen formation. Noncollagenous protein shares 10% of organic matrix in bone. However, only two of these noncollagenous proteins are unique to bone. Some are more abundant in bone than other tissue. The current role and function of these proteins are still poorly understood.

Proteoglycan is a special class of glycoprotein which is the combination of a core protein and one or several glycosaminoglycan. Glycosaminoglycan is a long, linear, carbohydrate chains which composed of various sulphated disaccharide subunit. It is highly hydrated macromolecules and has large volume. The current function of proteoglycan is still unknown; it may be involved in space reservation for future bone matrix deposit (Robey PG, 1994).

Glycoprotein is composed of covalently bonded polypeptide backbone and oligosaccharide chains. Phosphorylation and sulphation of protein is common. Common glycoproteins present in bone are osteonectin, integrin, vitronecin, osteopontin, fibronectin, thrombospondin etc (Robey PG, 1994). Some of them contains the arginine-glycine-aspartic avid cell attachment sequence and are expected to be involved in cell adhesion.

Bone has four main types of cells which are known as Osteoprogenitor cells, osteoblast, osteoclast and osteocyte. Osteoprogenitor cell is undifferentiated stem cell which can give rise to osteoblast. Osteoblast is responsible for bone matrix deposition. Mature osteoblast is highly polarized with a prominent Golgi apparatus which is a typical feature of highly secretory cells (Marks SC and Odgren PR, 2002). It can produce protein like type 1 collagen and noncollagenous proteins such as proteoglycan, osteopontin, osteocalcin, bone sialoprotein which are very important for bone matrix deposition. One of the postulated bone matrix formation mechanisms is the secretion of lipid matrix vesicle which allows calcium and phosphate to crystallize. Then it is attached on the collagen and form a nucleation site for mineralization and hydroxyapatite formation.

Osteocyte is differentiated osteoblast trapped in lacuna. It is characterised by long, dendritic-like processes which interconnects other osteocytes through canuliculi. It consists of 90% of cell in bone. Traditionally, osteocyte is expected to be mechanosensitive. It role is the detection the bone damages and activation of bone remodelling (Noble BS et al, 2003). In new theory, osteocyte may be involved in bone remoulding inhabitation. If loading to bone is reduced, the generation of inhabitation signal from osteocyte will decreases and subsequently activates the remoulding activity of osteoblast (Burr D., 2002). If excess loading or bone damages occur, it will form microcracks and cause osteocyte to undergo apoptosis. This will reduce the generation and transmission of inhabitation signal again and activate the bone remoulding.

Osteoclast is a multinucleate cell with 6-8 nuclei typically. Its diameter can range from 20 to several hundred microns. It is derived from fusion of hemopietic cells

from macrophage-monocyte lineage (Gay CV., 2005). They have abundant carbonic anhydrase which supplies hydrogen ion to the proton-ATPase. This is important for the acid production to digest the calcium phosphate salt in bone during the bone resorption process. It also forms a ruffled border and attached on the spicule of bone in the present of osteopontin and other RGD-peptides. This process is known as bone resorption.

2.1.2. Bone repair and regeneration solution

To repair or replace a large part of defected bone tissue, such as large defects and serious fractures, transplantation is a common clinical practice to assist healing of tissue (Kaduyala S et al., 1994). Bone graft and other non-living implantation are commonly applied for this purpose.

2.1.2.1. Bone graft

The main sources of living transplantation are autologous graft, allogenic graft, isogenic graft and xenogenic graft from healthy donors. However, the graft harvesting requires surgery which is an invasive procedure. The supply is limited to avoid site morbidity (Habibovic P and de Groot K., 2007). For autologous graft, it is even more risky to donor, especially when the donor is in a bad condition that requires transplantation. The supply of autograft is limited. Isogenic graft is possible for identical twins only. Even identical twins' tissue is genetically identical and has no risk of immune rejection; it may still cause disease transmission from donor to receiver. Allogenic graft requires a strict tissue selection to avoid immune rejection. Disease transmission is another risk. The current application of xenogenic graft is very limited. It may also cause immune rejection, disease transmission across different species. Ethical issue is another problem needed to be solved (Burgess EA and Hollinger JO,

1998). Besides the stated problems, there are some common weaknesses against the use of graft. Complications or non-union are common inconveniences, especially for large reconstruction (Cancedda R et al., 2007). Incomplete substitution is another common problem and resulted in late graft fracture. According to Wheeler and his co-workers' study (2001), 60% of allogenic graft receiver suffered from late graft fracture in 10 years. Therefore, more study is required to address the above problems.

2.1.2.2. Non-living implantation

Besides living bone graft, non-living implantation, such as metallic or polymer implantation is another popular solution. Unfortunately, metal or polymer is nonviable and doesn't have self-repairing ability. It will loosen and deteriorate gradually after daily use. The debris produced from wear-and-tear and surface corrosion may also cause inflammation. For metal-on-metal articulation implant, it produces $6.7x10^{12}$ to $2.5x10^{14}$ particles every year. It is 13,500 times of particles produced by metal-on-polyethylene bearing (Keegan GM et al., 2007). However, the particle size of metal-on-metal implant is generally less than 50nm, which is much smaller than the metal-on-polyethylene implant, which is rarely less than 100nm (Keegan GM et al., 2007). Dissolution of metal ion occurs at all metal surface. These metal ions may alter the chemical and biological environment. For metal particles less than 150nm, it may be uptake by the cell through non-specific receptor-mediated endocytosis and pinocytolysis. For particles larger than 150nm, they may be uptake by phagocytosis (Keegan GM et al., 2007). If the debris is engulfed by macrophages, it results in release of RANKL. This will activate the osteoclasts and causes bone resorption (Verhaar JA., 2007). The internalization of these metal ions may induce cytotoxicity, chromosomal damage and oxidative stress. Co(II),

Ni(II) and Cr(VI) ions released by metallic implants have been found to damage DNA, protein and lipids, inhibit DNA repair, alter signal transduction and gene expression. Cr(III) has also been found to be a potential mutagenic chemical. Co(II) and V(III) are found to be cytotoxic and cause necrosis and apoptosis in a range of cell. Titanium ion can also result in oxidative damage to DNA (Keegan GM et al., 2007).

For non-living implantations used to substitute mechanics-sensitive tissue such as bone tissue, the incompatibility in mechanical properties between implant and bone may cause stress shielding. Most weight-bearing non-living implant requires secondary operation and replacement after certain years. From the revision study done by Crawford RW and Murray DW (1997), they found that revision surgery occurs at a rate of approximately 1% per year for the first 15 years. Acetabular component loosening, infection, technical errors at the time of surgery, and recurrent dislocation are common reasons for the revision. Therefore, secondary operation may be required to fix the loosened implant.

2.1.2.3. Engineered tissue

Since there are so many weaknesses and drawbacks for bone graft and non-living implantation, tissue engineering, which engineer artificial tissues from receiver's cells, can be a good alternative to address these problems. Tissue engineering can be defined as 'the application of the principles and methods of engineering and the life sciences toward the fundamental understanding of structure-function relationships in normal and pathological mammalian tissues and the development of biological substitutes or bridging materials that restore, maintain, or improve tissue function'

(Patrick CW Jr et al., 1998). Since tissue contains numerous cell and factor distributed in three-dimensional space, stimulation of the microenvironment is required for tissue culture (Yang Y et al., 2005). Biomaterials provide a 3D framework for cell proliferation and cells are responsible for tissue production. They are used together for development of biological tissue substitutes. Since the engineered tissue is produced from receiver's cell, they are genetically identical and don't have immune rejection. It also requires small number of cells; it is less risky to be the cell donor than tissue donor. The current sterilization technique and culture equipment can culture tissue in pathogen free environment. This reduces the possibility of disease transmission. The engineering of tissue can be highly speeding up when the technology is mature. It may also produce tissue in specific shape by careful scaffold design. The engineered tissue is living and self-repairing, it can be incorporated into the defect tissue as a permanent solution. This provides the best solution for function restoration.

2.2. Biomaterials and carbon nanotubes

In order to engineer the living tissue, inducing the proliferation and differentiation of cell is very important. To mimic the in vivo environment, biodegradable polymeric biomaterial has been used to build biocompatible scaffold for cell proliferation, cell differentiation and loading transmission.

2.2.1. Biodegradable polymeric biomaterial

2.2.1.1. Natural biodegradable polymer

Bovine/human serum albumin, collagen, gelatine, chitosan, alginate and haemoglobin are natural biodegradable polymeric biomaterial. They are non-toxic and

immunologically tolerable. They have been investigated for the potential use for tissue engineering. Unfortunately, it is common that they have low purity, high immunogenicity and high cost (Maysinger D and Morinville A., 1997). Unless these issues have been solved, they are currently not the best material for the application in tissue engineering.

2.2.1.2. Synthetic biodegradable polymer

Poly (Lactic acid) (PLA) is a common biomaterial for bone tissue engineering (Yuan et al., 2001). PLA, that is a member of the α-hydroxyl acid family, and can be synthesized by ring-opening polymerization of cyclic diesters lactide. PLA has two enantiomeric isomers known as PLLA and PDLA. PLLA has higher crystallinity and has a slower degradation rate (Marra KG, 2005). Non-specific hydrolytic scission is the primary mechanism of degradation of PLA. Hydrolysis of ester linkage occurs and breaks the polymer chain into smaller chain. Then the monomer, lactic acid is metabolized in tricarboxylic acid cycle. It is one of the synthetic biomaterials approved by Food and Drug Administration of the United States. The current application of PLA and Poly (Glycolic acid) (PGA) is wide and highly versatile. It has been applied in many biomedical area such as degradable sutures, skin grafts, absorbable sutures, screws, pins, controlled drug delivery, orthopaedic and reconstructive implants, scaffold for bone, cartilage and meniscus engineering (Maysinger D and Morinville A., 1997; Agrawal CM and Ray RB ., 2001; Marra KG, 2005).

In drug delivery, Even though various natural and synthetic biodegradable polymeric biomaterials have been discovered, they have certain weakness and limitation

in the biological application. For examples, bovine/human serum albumin, collagen, gelatine and haemoglobin have been found unsuitable for drug delivery due to their high costs and impurity. Synthetic biomaterials, like lactide and glycoside, don't have the weaknesses associated with natural polymeric biomaterial. They also bear some good characters and make them more attractive then natural biodegradable polymer. They have good mechanical properties, predictable biodegradation kinetics, excellent biocompatible and low immunogenicity. 125 μm sized PLGA microparticle has been found suitable (Jain RA, 2000).

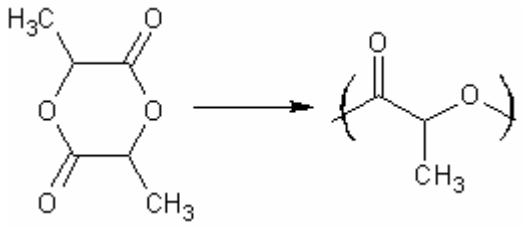

Figure 2-1 Schematic diagram of polymerisation of lactide.

It has many good properties that highlight it to be an attractive material for tissue engineering. It has good mechanical strength, biodegrading properties, low toxicity and low immunogenicity (Yamaguchi M et al, 2004). PLA has comparable mechanical strength as cortical bone. It can be a temporarily support towards bone defect. When it is being implanted, it will be gradually depolymerised by hydrolysis and body metabolism. Finally it can be completely replaced by regenerated tissue. Many studies have been done on the characterisation of PLA and its copolymer (Shi et al., 2002). Its mechanical and biodegradable properties can be further fine-tuned by forming co-polymer such as PLA/PGA. It provides further malleability by forming porosity structure known as scaffold and allows the incorporation of or coating with bioceramic and protein (Liao et al., 2004; Rizzi SC et al., 2000). This can make PLA to become osteoconductive. Both

physical porous structures and chemical factor enhance the cell seeding, cell adhesion and cell proliferation.

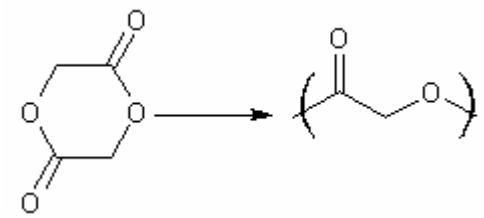

Figure 2-2 Schematic diagram of polymerisation of glycolide.

Poly (glycolic acid) (PGA) is another common biomaterial used together with PLA for bone tissue engineering (Yuan et al., 2001). PGA, similar to PLA, is a member of the α-hydroxyl acid family, and can be synthesized by ring-opening polymerization of cyclic diesters glycolide. PGA has general low solubility among common organic solvent except hexafluoroisopropanol (Marra KG, 2005). Hexafluoroisopropanol is highly toxic and is not commonly use in PGA processing. In stead, extrusion method is more common to make PGA in fibre form. Non-specific hydrolytic scission is the primary mechanism of degradation of PGA. Hydrolysis of ester linkage occurs and breaks the polymer chain into smaller chain. Then the monomer, glycolic acid is metabolized either by hydrolysis of ester linkage or by nonspecific esterase and carboxypetidase, or excreted through urination. It is one of the synthetic biomaterials approved by Food and Drug Administration of the United States. It has been applied in many biomedical area such as scaffold for bone, cartilage and meniscus engineering (Agrawal CM and Ray RB., 2001).

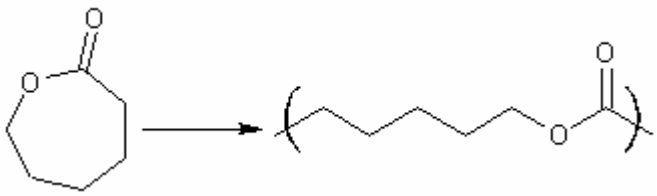

Figure 2-3 Schematic diagram of polymerisation of caprolactone.

Poly(ε-caprolactone) (PCL) is another potential material for tissue engineering. It is also a regulatory approved biocompatible polymer and has been applied in drug delivery system (Ciapetti et al., 2003). It has low glass transition temperature at -60 ^{o}C and maintains a rubbery state at room temperature. It also has high permeability and has been investigated for application in drug delivery (Coombes AGA et al, 2004). It has slow resorption time more than two years (Pitt et al., 1990). To shorten the degradation period, copolymerization with lactic acid was successfully demonstrated. The weak mechanical properties of PCL have also been improved by reinforcing with phosphate glass fibre (Coombes et al., 2004) and hydroxyapatite (Ciapetti et al., 2003). Coating of fibrin has been done by Pankajakshan D and his colleagues (2007) and shows an improved cell adhesion, spreading, proliferation and viability. However, the tensile strength of PCL (MW: 44,000) is only 57% of L-PLA (MW: 50,000). Therefore, if the mechanical strength of PCL can be improved, it is highly potential biodegradable polymer for bone tissue engineering.

Polydioxanone is a colourless, crystalline and biodegradable polymer formed by catalytic polymerization of monomer paradioxanone. It has low glass transition temperature between -10 to 0 ^{o}C. It has been used as a suture. It has high elasticity, high strength and slow resorption rate (Boland ED et al., 2005). It is an attractive material and is being used in, orthopaedics, plastic surgery, drug delivery, cardiovascular applications, and bone repair applications (Boland ED et al., 2005). However, it has a faster degradation rate than PLA, which may be undesirable to slow healing and load-bearing tissue.

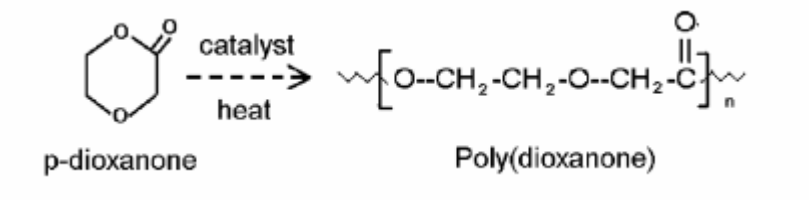

Figure 2-4 Schematic diagram of polymerisation of p-dioxanone. (Boland ED et al., 2005)

Poly (ethylene glycol) diacrylate (PEG) hydrogel is a water insoluble polymer with high water content. It has been widely investigated for potential in tissue engineering because of biocompatibility, tissue-like water content and 3D network structure (Xin AX et al., 2006). It can be fabricated into different shape, dimension and degradation rate by photopolymerization (Xin AX et al., 2006). Peled E and his coworker (2007) have successfully incorporated the fibrinogen into PEG. Some study shows that fibrin is osteoinductive and is a potential material to assist bone healing. It can be used in combination of other materials, such as hydroxyapatite and coral granules. However, other study shows that it may have some negative effect when using in combination of bony allograft, coral granules and bovine osseous graft (Peled E et al., 2007). More studies are required in order to figure out the positive effect and negative effect of PEG with conjugated fibrinogen. Jung RE and his colleagues (2007) have studied the RGD-modified PEG containing parathyroid hormone. It shows enhanced bone regeneration. However, more study is needed to understand its potential application in load-bearing region.

Figure 2-5 Structure of ethylene glycol.

Poly(propylene fumarate) is another attractive biomaterial for tissue engineering. It is linear polyester and can undergo ester bonds scission by hydrolysis (Lee et al, 2006). Besides biodegradability, the degraded product is non-toxic to the tissue. It is also injectable and allows in situ cross-linking. It is also an injectable biomaterial and able to polymerized in vivo. However, it has weak mechanical strength that is comparable to trabecular bone only (Peter SJ et al., 1997). Addition of bioceramics, such as β-tricalcium phosphate (Lee et al, 2006) and single-walled carbon nanotubes (Shi X et al., 2007) have been success and further enhanced its mechanical strength.

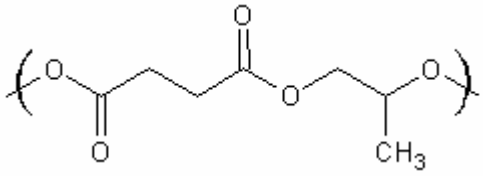

Figure 2-6 Structure of poly(propylene fumarate).

Poly(trimethylene carbonate) is one of the polycarbonate-based polymers which has been studied for potential tissue engineering. It is an aliphatic polymer and undergoes degradation in physiological condition. However, it is extremely soft at 40-60 ^{o}C and may not be a good candidate for bone tissue engineering. Another commercial available polycarbonates, poly(BPA carbonate) has high mechanical strength and is more stable than poly(trimethylene carbonate). But it loses nearly all physiological degradability and is not suitable for making biodegradable scaffold.

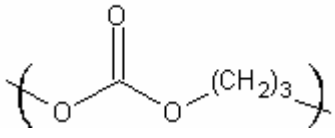

Figure 2-7 Structure of poly(trimethylene carbonate).

Even poly(lactic acid) (PLA), poly(glycolic acid), poly(ε-caprolactone), and their copolymers have attracted wide attention for their biodegradability in the human body. However, the mechanical strength, toughness, and elastic modulus of these polymers were lower than those of natural cortical bones when fabricated in form of scaffold. Thus, for preparing a desired material that presents high mechanical performance to match natural bones, inorganic fillers were introduced into biodegradable polymers to fabricate filler/polymer composites, such as hydroxyapatite (HAP), tricalcium phosphate etc (Miao X et al., 2008). Carbon nanotube, which poses excellent mechanical properties, would be investigated for the application of polymer reinforceement.

2.2.2. Carbon nanotubes

Carbon can form numerous allotropes because of its unique atomic structure. Some examples are diamond, graphite, fullence etc. Carbon nanotube is a member of fullence family which is a cylindrical form of grapheme sheet. The grapheme sheet is composed of hexagonally-boned carbon. The bonding between carbon atoms is strong sp2 bond. Since sp2 bond is very strong bond, carbon nanotube has superior mechanical strength. Carbon nanotubes can be further catalogued into single-walled carbon nanotubes and multi-walled carbon nanotubes. Besides, carbon nanotubes can be chemically modified to incorporate some functional groups, such as carboxylic acid group, fluorine, nitrenes etc (Chen et al., 2005). This great prospect of carbon nanotubes attracts much attention in research of biomaterial reinforcement and tissue engineering.

Carbon nanotubes were discovered by Iijima (1991). It demonstrates a lot of unique properties and receives attention after the discovery. One of the most attractive features of carbon nanotubes are high mechanical strength. It shows that carbon

nanotubes can be a potential element to reinforce other material. Some studies have been conducted and proved that carbon nanotube can be incorporated and bonded with PLLA successfully (Chen et al, 2005 and Zhang et al, 2006). It has also been evaluated to seek the potential application in different four areas – cell tracking and labelling, sensing cellular behaviour, augmenting cellular behaviour and enhancing tissue matrices (Harrison B.S and Atala A., 2007)

To build biomaterial/carbon nanotube matrix, one of the challenging question is carbon nanotube dispersal. Since carbon nanotubes have strong van der Waal's interaction and strong inter-nanotubes anisotropic interaction (Li Q et al, 2005), they would like to aggregate into tangled networks. This problem is further worsened by its high length to diameter ratio. This will create uneven distribution in biomaterial matrix and may influence the degree of properties expression of each carbon nanotubes. This is a limitation to the application of MWCNT in composite fabrication. To solve this issue, several methods have been proposed to disperse carbon nanotubes. Chemical oxidation has been proposed to separate carbon nanotubes. Carbon nanotubes can be treated with oxidizing agent like concentrated HNO_3 and H_2SO_4 to oxidize the CNT. Functional group will be introduced to the side chain on carbon nanotube wall. Functionalized MWCNT can further be processed to bond other organic molecules by esterification or amidation. The repulsion between added functional group can help dispersing the MWCNT and reduce aggregation. However, chemical modification may alter some important properties of the CNT. Damages to MWCNT structure is another undesirable effect which make chemical modification unsuitable. Physical separation can also be done by adding dispersing agent. Polysaccharide like Gum Arabic (Rajdip et al., 2002), polymer likes poly(diallyldimethylammonium chloride) (Li d et al., 2003),

Diazapentacene Derivative (Aurelio MA et al., 2007), poly(acrylic acid) and poly(allylamine hydrochloride) with pH adjustment (Grunlan JC et al., 2007) and sodium dodecyl sulphate and Triton X-100 (Islam MF et al, 2003). They have been found to be an effective dispersing agent to CNT. This dispersing agent will adsorb on MWCNT and prevent aggregation. However, they are difficult to remove and may contaminate the CNT. This causes a problem when a clean, pure and thoroughly dispersed MWCNT is needed. Li Q et al (2005) demonstrated the use of ethanol-NaOH solution containing 105g of NaOH in 80% volume of ethanol and 20% of water to disperse the SWCNT after 5 hours of sonication. This may provide another good method to disperse MWCNT as NaOH, ethanol and water can be easily removed to obtain pure MWCNT. Chen GX et al (2005) reported the use covalent modification of CNT to PLLA polymer. It has been observed that the amount of CNT attached to PLLA is inverse relationship to the molecular weight of PLLA. This may suggest another way to distribute CNT on a polymer thoroughly on PLLA with low molecular weight. To solve this issue, sonication has been found to be a good solution which requires no chemical addition and chemical reaction. To overcome the strong van der Waal's interaction, a very high power of ultrasound wave is required to overcome the interaction. Too low power will result bad MWCNT dispersion and too high power may damage the MWCNT structure. Yang DQ et al (2005) demonstrated the use of sonication to disperse MWCNT in deionized water. The MWCNT sonicated for 45 min shows a stable dispersion after 3 weeks.

There are some controversies about the biocompatibility and cytotoxicity of single-walled carbon nanotubes and multi-walled carbon nanotubes. From some in vitro studies, some studies show that CNT are cytotoxic while other studies show that CNT

has no adverse effect on cell growth. However, since different scientist uses different length, different diameter, different concentration and different allotrope of CNT, and different cell type, it is very difficult to conclude if the whole family of CNT is 100% cytotoxic or biocompatible. According to the study by Jia G et al (2005), they found that SWCNT in 1.4nm diameter and mean length of 1 μm and MWCNT in 10-20 nm diameter and 0.5-40 μm length are cytotoxic to alveolar macrophage. According to the study carried out by Shvedova AA et al (2003). Single-walled carbon nanotubes seems cytotoxic to the immortalized human epidermal keratinocytes (HaCaT) after 18 hour of exposure. Formation of free radicals, increase in peroxidative compound, antioxidant depletion and dead cell were observed. Cui D et al (2004) studied the effect of SWCNT on human HEK293 cells. The result shows that SWCNT can inhibit the proliferation of HEK293 cells, inducing cell apoptosis and decreasing cellular adhesion ability. When 100μg/ml of SWCNT was added into the culture medium, 64.8% of cell undergoes apoptosis after 72 hours. When the dose of SWCNT increased to 150μg/ml, it resulted in 78% of apoptotic cell after 72 hours. Pantarotto D et al (2004) used FITC-labeled single-walled carbon nanotubes with 1nm diameter and 300-1000nm in length to study the effect on fibroblast. They found that 5 μM of CNT can keep 90% of fibroblast alive while 10 μM of CNT can keep 20% of fibroblast alive. Lu Q et al (2004) conjugated the SWCNT with RNA polymerase (in ~1.4 nm diameter and 400nm long) and uses MTS assay to evaluate the cytotoxic effect on MCF7 breast cancer cells. The result showed that, up to 0.5 mg/ml concentration of SWCNT, there is negligible cytotoxic effect on MCF7 cells. Cherukuri et al (2004) studied the effect of SWCNT on mouse peritoneal macrophage-like cells. 1 nm average diameter and 1 μm average length of SWCNT were used. He concluded that there is no morphology, adhesion and confluence

comparing with the control experiment when culturing cell with 3.8 μg/ml of SWCNT. Bianco A et al (2004) concluded that ammonium-functionalized SWCNT has no toxic effect on mitogen activated (ConA, Conconavalin A) and nonactivated mouse splenocytes.

2.2.3. Importance of mechanical environment and surface properties

2.2.3.1. Bone remodelling

The current understanding of structure-function of bone tissue is limited. Woff's law explained that bone is a dynamic structure and adjusts itself when subject to change of loading (Hill, 1998). According to the study carried out by Basso N and Heersche JNM (2002), bone cell can sense the load and modify the bone structure in a feedback mechanism. Even the details of the exact cellular activation pathway of bone remodelling are not clear, it has been shown that bone cell differentiation was stimulated by repeated loading (Altman et al., 2002). After repeated loading, the formation of microcracks was suspected to be the first signal for bone remodelling (Taylor D et al., 2003). Some studies show that strain can affect the proliferation, synthetic activity and enzymatic activity of bone cells (Basso N, Heersche JNM, 2002), but not the rat osteoclasts in hemiepiphyses significantly (Pazzaglia et al., 1997). This suggests that mechanical loading is likely to be an important factor to bone tissue regeneration. Direct mechanical stress or fluid shear stress alter bone architecture and are found to be involved in the remodelling process. In vivo, bone requires 200-2000με strain to maintain equilibrium. However, excessive strain beyond 5000με is pathological and result in bone damages (Basso N, Heersche JNM, 2002). The result is consistent with the result from Burr et al (1996) that tibial surface strain is below 2000με during

vigorous activity. Basso N and Heersche JNM (2002) also reported the active site of bone remodelling in different types of bone. In cortical bone, Haversian canel is the main site of bone remodelling and can reach 100-200μm wide and 10mm long. In cancellous bone, Howship's lacunae in 60-70μm depth and 0.1μm diameter will be formed; all of them will be refilled by osteoblast.

Even we have some understandings of the onset environment for bone remodelling, the actual cellular mechanism behind is still poorly understood.

2.2.3.2. Basement membrane

Surface properties of the basement membrane have been found to govern the cell behaviour. Chemically, it consists of many extracellular matrix components likes fibronectin and collagen. The mechanical properties, like tensile properties, have also been found to have effects on cell behaviour. This is especially important for load-bearing tissue. Physical topology, likes pores, ridges, grooves and steps are another factors which can affect cell response. Therefore, careful selection of material to simulate the basement membrane for cell cultures is important for tissue engineering.

2.2.3.3. Response of osteoblast towards biomaterial surface

The signal transmission system of the bone tissue depends on the integrity of the bone tissue. It may not function properly in case of severe bone damage. To regenerate and replace the defeat tissue, biomaterial scaffold may be used to facilitate the healing process. When osteoblasts land on a biomaterial surface, they will undergo cell adhesion,

migration, proliferation and differentiation. The cell will stretch itself and adhere itself on the substrate surface. Focal adhesions will be formed by connecting the actin filament of the internal cytoskeleton to interstitial matrix (Meyer et al., 2005). Apoptosis will occur if the cell is unable to achieve this stretched morphology. Therefore, the surface properties of biomaterial surface can be a major factor governing the viability and activity of the osteoblasts. Since osteoblast is mechanical-sensitive, the surface parameter of the biomaterial are expected to influence the proliferation and differentiation of cell. To study this parameter, the Young's modulus of the biomaterial is a good indicator of the mechanical properties.

2.2.4. Nanoindentation of Biopolymers

Nanoindentation techniques were developed based on the classic elastic contact problem as a testing technique to look at thin films on hard substrates. It offers the potential of highly directional mechanical tests, extremely light loads, small displacements and the ability to separate the mechanical behaviour of different constituents. In modern nanoindentation, the tip is attached to the centre plate of a parallel plate capacitor, which is extremely sensitive to small changes in z displacement. From the experimental data, one can calculate the reduced elastic modulus for the indented material using the method of Oliver and Pharr (1992) for an axisymmetric indenter (Oliver et. al, 1992). If the Poisson's ratio of the material is known, a value for the true elastic modulus can be determined. The solutions for indentation on hard, elastic materials are well known and can be used to estimate mechanical properties repeatably and with a reasonable amount of certainty. For thin films of elastic materials, the correlation with bulk materials properties is quite good.

According to the review by Oliver WC and Pharr GM (2003), hardness is defined as the maximum load P_{max} divided by the area of contact,

$$H = \frac{P_{\max}}{A(h_c)}$$

and the reduced modulus is calculated using the following equation,

$$E_r = \frac{\sqrt{\pi}}{2\sqrt{A(h_c)}} S$$

where S is the measured contact stiffness at initial unloading, and $A(h_c)$ is the contact area as a function of contact depth h_c. The tip area function is calibrated by indenting on a standard fused silica sample. The reduced modulus is a property that accounts for elastic deformations in both the material being indented and the indenter and is defined by:

$$\frac{1}{E_r} = \frac{1-v_i^2}{E_i} + \frac{1-v_s^2}{E_s}$$

Where v_i and E_i are the Poisson's ratio and Young's modulus of the indenter, and v_s and E_s are the same parameters of the sample (Oliver WC and Pharr GM, 2003).

2.3. Cell Response

In order to study the interaction of cell and biomaterial surface in detail, biomaterial film of different stiffness, surface pattern and surface coating will be prepared and seeded with human osteoblast-like cells (osteosarcoma). Human osteoblast-like cell are found to be more homogeneous, phenotypically stable and easy to propagate and maintain relatively (Meyer U et al., 2005). The cell shape, cell morphology, cell metabolism, osteoblast differentiation markers such as alkaline phosphatetase activity, focal adhesion marker (vinculin) and changes in cytoskeleton

morphology will be studied and monitored. The result will be compared with cells growing on pure PLLA surface.

2.3.1. Cell metabolism

Mitochondrion is the power house inside the eukaryotic cells and is responsible for ATP production. It consists of various enzymes which are responsible for step in glucose oxidation. In aerobic respiration, glycolysis, Krebs cycle and electron transport system are the main steps for the whole glucose metabolism. Mitochondrial dehydrogenase is one of the enzymes found in the inner membrane of mitochondrion and is involved in electron transport system. When the cell activity increases, the demand for ATP increases. The increase in ATP demand will finally increase in mitochondrial activity for ATP production. 3-[4,5-dimethyl-thiazol-2-yl]-2,5-diphenyltetrazolium bromide (MTT) is one of the substrate for mitochondrial dehydrogenase in yellow colour. When MTT is reduced by mitochondrial dehydrogenase, it will form insoluble tetrazolium salt inside the cell. By monitoring the amount of purple tetrazolium salt produced, the rate of cell metabolism can be monitored.

2.3.2. Alkaline phosphatase

Alkaline phosphatase is an enzyme found inside all human cells. However, high concentration was found inside the cell in bone, liver, kidney, placenta etc. In osteoblast, alkaline phosphatase is involved in the removal of nucleation inhibitor to promote calcium crystal formation in matrix vesicle (Sikavitsas et al., 2001). It is an important index of osteoblast differentiation (Kapur S et al, 2005).

2.3.3. Focal adhesion protein

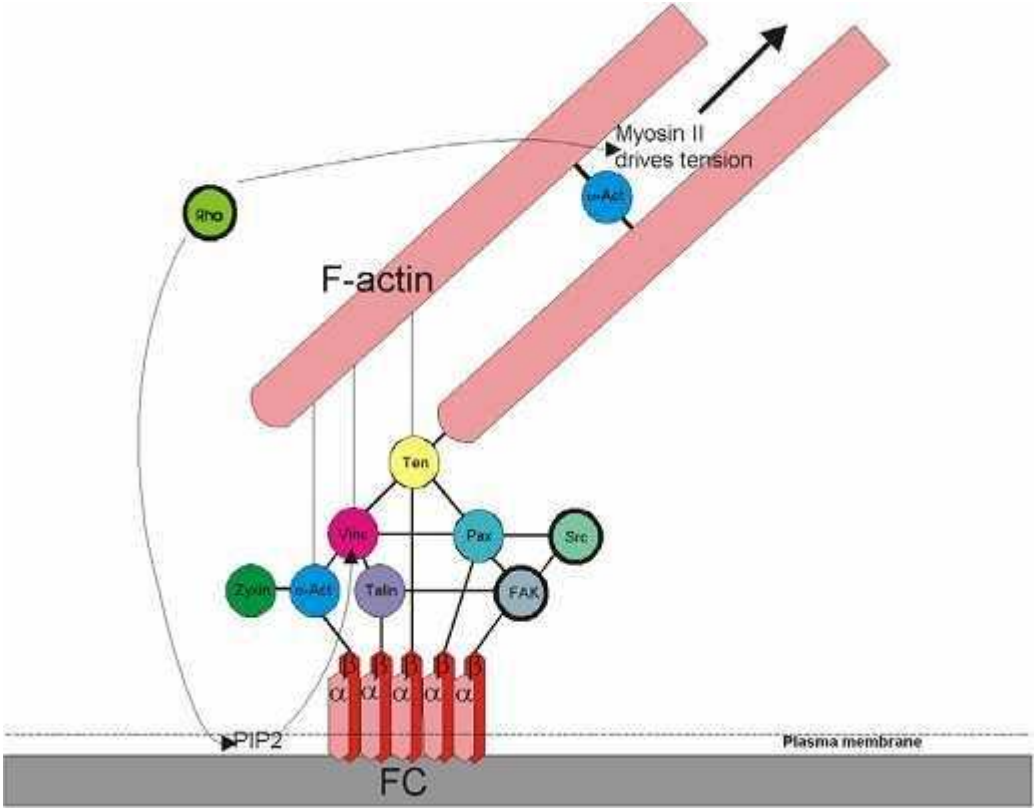

Figure 2-8 Interaction of the most focal adhesion linker and signalling protein. (Owen GRh et al., 2005)

Cell adhesion is a prerequisite for further cell activity such as spreading, proliferation and differentiation; it is the most important early stage of cell interaction (Rizzi SC et al, 2000). The cell adhesion can be divided into protein adsorption to material surface, cell contact, cell attachment and cell spreading. After cell adhesion, cytoskeleton reorganization, and cell flattening will be followed. Focal adhesion, which will be formed during cell adhesion, will be observed at the cell binding point on the biomaterial surface. Focal adhesion was also strongly related to cellular signal transduction. It is composed of a high density of proteins that bridge the excellular portion of cell to the intracellular cytoskeleton portion (Figure 2-8). Integrin is the transmembrane protein found in cell membrane. It attached to extracellular matrix and connected them to intracellular actin filament through many pathways (Meyer U et al.,

2005). One of the pathways is through talin-vinculin-tensin. The signal can be relayed to cell nucleus and affect the gene expression (Juliano, 2002). Since integrin composes of two subunits and the β subunit has eight heterodimers, it is difficult to monitor different kind of heterodimers comprehensively. There are two types of focal adhesion named as dot and dash contact. Dot contacts contain vinculin and α-actinin only while dash contacts contain vinculin, α-actinin and other linker proteins. By monitoring morphology of f-actin in cytoskeleton, it can provide some information about the cell adhesion.

2.3.4. Scaffold fabrication method

2.3.4.1. Solution casting

Schmitz JP and Hollinger JO (1988) used solution casting to make scaffold using demineralised bone and PLGA. 50:50 PLGA copolymers was first dissolved in solvent. The solution was precipitated with addition of methanol and combined with demineralised freeze-dried bone. Then they were injected into a mould and kept at 45-48 ^{o}C for 24 hours. Singhal AR and his co-workers (1996) modified the experiment. They used acetone to dissolve 50:50 PLGA copolymer and ethanol to precipitate the copolymer. A telfon mould was used to mould the polymer under vacuum. A scaffold with low porosity (40-50%) was formed.

2.3.4.2. Gel casting

Gel casting is a scaffold fabrication method reported by Coombes AG and Heckman JD (1992). They used solvent like acetone to dissolve the polymer. The solution was poured into a mould and left it in room temperature. When the solvent was

partially evaporated, the polymer was become a gel. The gel was extracted by several steps of solvent exchanges to form a porous solid implant. This method has the advantage of low processing temperature; however, it is not popular scaffold fabrication technique. Its complex process and other simpler low temperature technique may be the reason.

2.3.4.3. Solvent casting and particulate leaching

This method requires the use of porogen and polymer to produce porous scaffold. Common porogen includes salt particulate or parafilm sphere. The porogen is first sieved to obtain particlulate in a specific size range. Organic solvent, which can dissolve the polymer but not the porogen, was added to dissolve the polymer of interest and mixed with the porogen. Then after the removal of solvent, the porogen is embedded inside the solid polymer. Then another solvent like deionized water, which can dissolve the porogen only, was used to leach out the porogen. This leaves a sponge of scaffold with pore size of the porogen (Mikos AG et al., 1993). Mikos AG and his co-workers (1993) have reported this method to produce PLGA scaffold by NaCl salt and chloroform solvent. Several layer of scaffold was laminated to give a 3D scaffold.

2.3.4.4. Gas saturation

This method has been used to fabricate PLGA scaffold by Mooney DJ and his colleagues (1996). A PLGA disc was first prepared and processed in a chamber with high pressure CO_2 gas (5.5MPa) at room temperature. After 72 hours, some CO_2 gas has been dissolved in the PLGA disc. Then the CO_2 gas pressure was rapidly reduced to

atmospheric pressure. This causes the expansion of CO_2 gas dissolved in PLGA disc and forms gas cells. The expansion of gas cell makes the PLGA spongy and gives 93% porosity with pore size around 100 µm.

2.3.4.5. Foaming

It is another method to produce porous scaffold. Bicarbonate salt is mixed with weak acids to generate CO_2 gas. This gas will form small bubbles and leave pore in the polymer during the polymerization reaction. It has been successfully used to generate pores at size range from 50 µm to 500 µm (Kim et al, 2007). Kim et al (2007) explained that this technique has higher protential use in injectable biomaterial as it won't create a hypertonic environment as salt leaching technique.

2.3.4.6. Gas foaming and particulate leaching

This method is a modified gas saturation method by Harris LD et al (1998). PLGA copolymer (85:15) and NaCl particulate were mixed and compression moulded by a KBr die at 1500psi for 1 minute at room temperature. The PLGA/NaCl disc (3.4mm thick) was transferred into a chamber with high pressure CO_2 gas (800psi). The polymer was slowly fused and embedded the particulate. When the polymer was saturated with CO_2 gas after 48 hour, the chamber pressure was rapidly released to atmospheric pressure and allows the nucleation of CO_2 gas to form gas cell. The particulate was leach out by deionizd water for 48 hours and give a marcoporous scaffold up to 96% porosity. Harris LD and et al (1998) conclude that this method can create scaffold with open-pore on the surface, which is not being observed in traditional

gas saturation method. The fabricated scaffold also has nearly double mechanical strength than scaffold fabricated by solvent casting and particulate leaching method with the same porosity.

2.3.4.7. Lyophilization

Hsu et al (1997) reported the success use of lyophilization of frozen polymer solutions to fabricate low-density PLGA, PBLG and PLGA/PPF foams in either glacial acetic acid or benzene solvent. The polymer was first mixed with solvent to give a solution. Then it was kept freezed at -10 ^{o}C and transferred into a ice bath under vacuum of <1mmHg for at least 7 days. The macroporous scaffold was formed after all solvent has been removed. Hsu et al (1997) also report that morphology of the foams fabricated was found to be related to the solvent type during the fabrication process. A capillary structure was observed when using benzene solution while a leaflet structure was observed when using glacial acetic acid. However, from the SEM image shown by the author, it shows that the pore is quite uneven. Optimization of this method is required to fabricate scaffold with better controlled pore size.

2.3.4.8. Three dimensional printing

The scaffold was constructed using CAD software. A modified cartridge, which is filled with the binder for monomer, was fitted into the printer. Then a chamber filled unbound powder was placed below the nozzle of the printer. When the nozzle reached the surface that requires polymer deposition, it ejects the liquid binder to the powder surface and join the powder. After finishing a layer, the base of the chamber was

lowered and filled with new layer of powder. The whole process was repeated until the whole scaffold has been constructed.

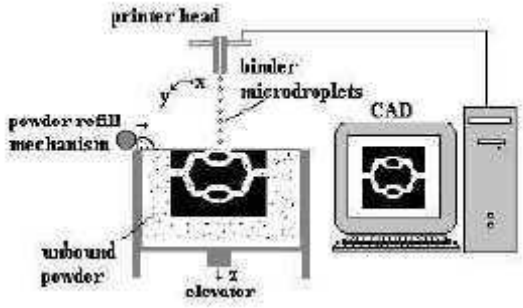

Figure 2-9 Schematic diagram of the 3-dimensional printing system. (Sachlos E and Czernuszka JT, 2007)

2.3.4.9. Phase-change printing

To produce scaffold using three dimensional printing, a model need to be generated. Lee et al (2006) has used SolidWork (SolidWorks Corp., Concord, MA) to create a scaffold model with 300 µm, 600 µm and 900 µm pore size. After the creation of the model, the model was converted into CAM format. The scaffold was then fabricated by the phase-change ink-jet printer. Then the building material was removed and leaving the supporting material. Then the biomaterial was dissolved and injected into the mould. Finally, the supporting material was removed and leaving a fabricated scaffold. This method provides better control of interconnectivity of channel in the scaffold (Lee et al., 2006).

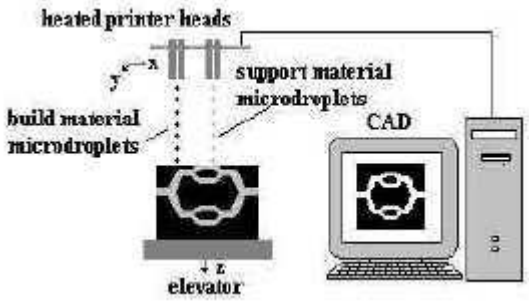

Figure 2-10 Schematic diagram of the phase change printing system. (Sachlos E and Czernuszka JT, 2007)

2.3.4.10. Stereolithography

This method was patented by Hull C (1990). Similar to 3D printing technique, this method requires the use of CAD program to construct the 3D pattern of the scaffold. However, an ultraviolet laser is used instead of printer. A layer of monomer was first deposited on a flat surface; they were irritated by ultraviolet laser according to the cross-section of the CAD pattern. This allows selectively polymerisation of the photosensitive monomer. When the first layer is complete, the next layer of monomer was deposit and the whole process was repeated. When the model was constructed completely, the supporting, unpolymerized monomer was removed, leaving a porous scaffold. It should be noted that this method can only be used for photosensitive monomer only.

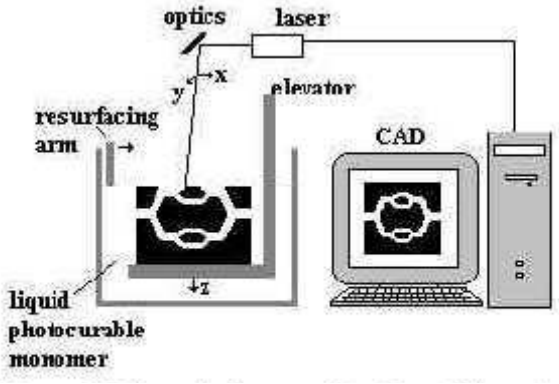

Figure 2-11 Schematic diagram of stereolithography system. (Sachlos E and Czernuszka JT, 2007)

2.3.4.11. Fused deposition modelling

Fused deposition modelling is a patented technique by Scott CS (1991). It is a dynamic fibre-extruding system which extrudes the fibre and fabricates the scaffold at the same time. In this system, a predefined 3D scaffold, engineer by CAD software, was transferred into signal to guide the nozzle of fibre extruder to deposit the polymer fibre. The scaffold was being built layer-by-layer. Even though the pore size of the scaffold fabricated by this method is sufficiently small, this method required the removal of unconnected fibre manually.

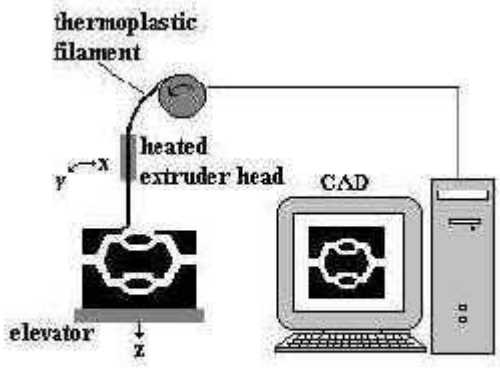

Figure 2-12 Schematic diagram of fused deposition modelling system. (Sachlos E and Czernuszka JT, 2007)

2.3.4.12. 3D Plotter

To plot the scaffold, the architecture of scaffold was first built by CAD program. Then a nozzle which can heat up the polymer into liquid form, was connected to compressed air (7 bar) to force out the melted polymer. When the nozzle reach the position that requires polymer droplet, the melted polymer was forced out. After the polymer droplet hit into a liquid medium or paste-like medium, it solidified. The whole process was repeated (11–12 m/h) until a complete scaffold had been built. The pore diameter was found to be 250 to 1500 μm.

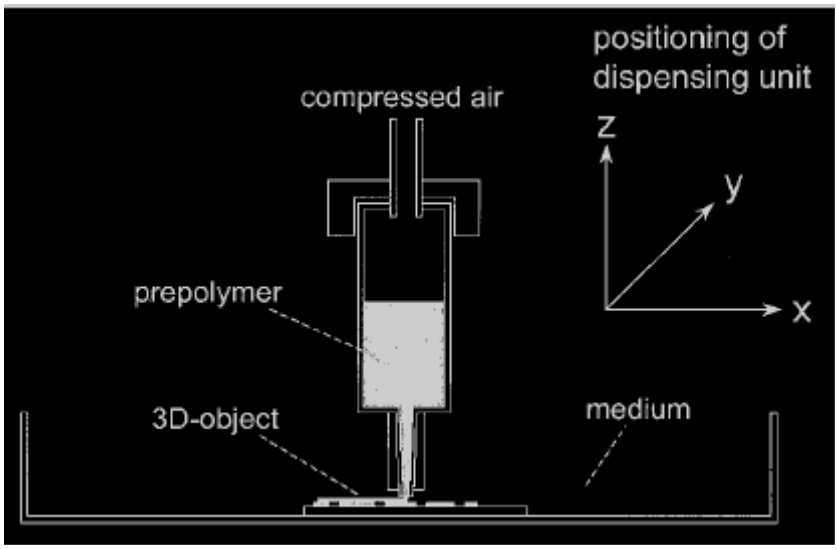

Figure 2-13 Schematic diagram of 3D Plotting system. (Landers R and Mulhaupt R., 2000)

2.3.4.13. Photolithography and microembossing

It is a popular technology in electronics fabrication. The 2D skeletal structure of the scaffold was printed on a mask. A supporting substrate, like silicon wafer coated with a layer of UV-sensitive photoresist, was exposed to the UV. The pattern on the mask was transferred onto the photoresist. The photoresist was hardened and formed a 3D skeletal structure after developing. The pattern was transferred into a rubber stamp, commonly fabricated by Poly(dimethylsiloxane). Then the rubber stamp was used to produce the skeletal stucture repeatedly using sacrificial layer embossing. After fabrication of enough skeletal structure, they were assembled into a 3D scaffold, by carbon dioxide bonding (Yang et al., 2004)

In this study, a method based on solvent casting and particulate leaching will be used as it doesn't require any thermoprocessing and special equipment

Chapter 3: Methodology

3.1. Fabrication of PLLA/Carbon Nanotube Composite

Poly (L-lactide) (PLLA) pellets (M_w =50, 000) were ordered from PURAC (Netherlands). Multi-walled carbon nanotube (MWCNT) (60-100nm diameter and 5-15 μm length) prepared by arc discharge method and purified by an acid-treatment process was ordered from Chengdu Organic Chemicals Co., Ltd, China. Different ratio of PLLA/MWCNT composite was prepared according to the data shown in Table 3.1. MWCNT was first added into Chloroform stabilized by ethanol (British Drug House, UK) and ultrasonicated with a high energy UP400S portable ultrasonic homogenizer (Ningbo Scientz Biotechnology Ltd, China) to break the agglomerates of carbon nanotube. The high energy ultrasonic horn oscillated the liquid and caused the nucleation and collapse of solvent bubbles. Bubbles initiating and collapsing on the solid surface effectively fractured the solids. The whole process was controlled by the specific energy input. The frequency of the ultrasound was kept constant at 24 kHz and 400W. To keep the dispersions from overheating during the ultrasonication, the dispersions were sonicated in a cold-water bath maintained at a constant temperature (10 ^{o}C). After 15 min. of sonication treatment, the stable black slurry of dispersed MWCNT was formed. Then PLLA was added into the slurry. Magnetic hotplate stirrer (Stuart Scientific, UK) was used to assist the dissolving of PLLA particles into chloroform under 25^{o}C at 120rpm for 12 hours. PLLA/MWCNT/Chloroform mixture was poured into a 10mm circular glass Petri dish with lid (Duran, Germany) and dried up in a fume hood at room temperature. After 96 hours, a punch was used to produce PLLA circular disc in 12.5 mm diameter. The films were stored in a desiccator.

Table 3-1 The composition of fabricated PLLA/MWCNT.

Amount of PLLA (mg)	400	395	390	385	380	375
Amount of multi-wall carbon nanotube (mg)	0	5	10	15	20	25
Overall weight ratio of multi-wall carbon nanotube (%)	0.00	1.25	2.50	3.75	5.00	6.25

Film was then sterilized by UV radiation for 1 hour. Sterile fibronectin from bovine plasma (F1141, Sigma-Aldrich) was diluted by PBS to reach a concentration of 10μg/ml. 250μl of diluted fibronectin was added to the film surface. The films were left dried in a biological safety cabinet (NU-425-400, NuAire) for 24 hours. The treated film was stored in tissue culture dish and kept at 4^{o}C.

3.2. Cell culture

3.2.1. Culture Medium Preparation

The medium was prepared by powder form of McCoy's 5A Medium Modified, with L-glutamine, without sodium bicarbonate (M4892, Sigma-Aldrich). 11.9g of medium powder and 2.2g sodium bicarbonate was dissolved in 800ml deionised water. The pH of medium was adjusted to pH 7.3 by addition of 0.1M HCl or 0.1M NaOH. Then additional deionised water was added to fill the solution to 900ml. The solution was filtered by a sterile, disposable vacuum filtration system with 0.22μm PES membrane (Stericup SCGP U10 RE, Millipore) in a biological safety cabinet. 100U/ml penicillin and 100μg/ml streptomycin (15140-122, Invitrogen Corporation), together with 10% foetal bovine serum (FBS) (16000-044, Invitrogen Corporation) were added to the filtrate. The medium bottle was sealed by parafilm and stored at 4^{o}C.

3.2.2. General Cell Culture

Human osteoblast-like cells (HTB-85, Saos-2) (HOB) was ordered from American Type Culture Collection (USA). They were stored in a liquid nitrogen tank. To begin the culturing of HOB cell, the cryovial was thawed in 37 ^{o}C water bath. When the whole content was melted completely, it was transferred into a 15ml centrifuge tube with 10ml of culture medium at 37 ^{o}C. The centrifuge tube was centrifuged at 2000RPM for 5 minutes and supernatant was removed. The cell pellet was re-suspended in 10ml culture medium and spread on a 100mm diameter tissue culture dish. (150350, Nunc). The tissue culture dish was transferred into an incubator (HERAcell 150, Heraeus) at 37 ^{o}C supplemented with 5% CO_2. Medium was refreshed every two days.

When the HOB cells reached confluence (~8.8x10^6 cells in Φ100mm tissue culture dish), the old culture medium was discarded. The cells were washed by 2ml 1x sterile, calcium-free phosphate buffered saline (cfPBS) (00-3002, Zymed) three times. 1ml Trypsin/EDTA (25200-056, Invitrogen Corporation) was added and the culture dish was placed into incubator for 10 minutes. The cell suspension was added into a 15ml centrifuge tube and centrifuged at 2000rpm for 5 minutes. The supernatant was discarded. 2ml fresh culture media was added. Continuous pipetting was carried out to re-suspend the cell pellet. 400µl of cell suspension, together with 500µl FBS and 100µl sterile dimethyl sulfoxide (DMSO) (0219605580, MP Biomedicals) were added into sterile cryogenic vial (8535, Stockwell). The vial was fixed on a cryocane (378441, NUNC) and stored in gaseous phrase in a liquid nitrogen tank for stocking. 500µl remaining cell suspension (~2.2x10^6) was spread on a new 10mm diameter tissue culture dish with 10ml fresh culture medium. The dish was eddied gently to distribute the cells evenly. The culture dish was incubated in the incubator. The culture cycle was repeated until enough stocks had been stored.

3.2.3. Cell Culture on PLLA/MWCNT Composite

HOB cells were cultured in a 24-well plate (142475, NUNC) with 1ml fresh culture medium. Culture medium was refreshed every two days. When the cells reached confluence in the well, each well was washed by 1ml 1X cfPBS three times. 0.5ml of Trypsin/EDTA was added into each well to digest the cells for 5 minutes at 37^{o}C. The cell suspension was centrifuged at 2000rpm for 5 minutes. Supernatant was discarded. 1 ml fresh culture medium was added to re-suspend the cell. Then they were transferred into a well with a sterile, fibronectin-treated film in a 12-well plate. The whole setup was cultured in an incubator at 37^{o}C and 5% CO_2. The medium was refreshed every two days.

3.3. Biomaterial characterisation

3.3.1. Scanning Electron Microscopy

Sample with different ratio of MWCNT was first fixed on an aluminum disc by conductive carbon tape. Additional silver paint was added to improve conductivity and reduced charging. The sample surface was sputtered with gold for 60 seconds. Then the gold-coated sample was transferred into the sample stage. Vacuum was applied to achieve 4.41x10^{-4}Pa. 3kV high tension, 10-12μA and 7.9-8.9mm working distance were configured for SEM imagining (Model JSM-6490, JEOL, Japan).

3.3.2. X-ray Diffractometry

Sample was fixed on a zero-background sample holding disc. Then it was fixed on a sample stage by vacuum (D8 Discover, Bruker AXS, Germany). Then the Z-axis machine was adjusted for maximum count. Theta-2-theta scan (Locked-couple) was

used to scan the sample from 10 degree to 50 degree at step 0.01 degree and 4 seconds per step. Cu Kα radiation at 40 kV and 40 mA was used. Nickel filter and 2mm slit was used for x-ray emitter. 0.6mm slit was used for x-ray detector. The data was saved as raw data. Background subtraction and peak search were done by DIFFRAC^{plus} EVA software (Bruker AXS, Germany).

3.3.3. Energy Dispersive X-ray Spectrometry

Sample with different ratio of MWCNT was first fixed on an aluminum disc by conductive carbon tape. The sample was transferred into the sample stage. Additional silver paint was added to improve conductivity and reduced charging. Then the sample was transferred into JEOL SEM Chamber (Model JSM-6490, JOEL, Japan) with EDX System (INCA x-sight EDS Detectors, Oxford Instruments, UK). Vacuum was applied to achieve 10^{-5} Torr. 10pA current was used during spectrum collection. The whole sample was scanned for 30 seconds to reach total 50 frames. C, O and Cl were labelled as element of interest by INCA Energy Microanalysis System software (Oxford Instruments, UK).

3.3.4. Nanoindentation

Nanoindentater (Nano Indenter IIs, MTS Systems Corporation, USA) was used to characterise the mechanical properties of the PLLA/MWCNT film. The film was first fixed on an aluminium sample holder by adhesive tape. It was placed inside the sample stage. A fine Berkovich tip was used to indent on the surface of polymer. It approached to the sample surface, loaded to the peak load, held the indenter at peak load, and then unloaded to 90% of the peak load in 30s, and finally, unloaded completely. Depth of penetration and maximum load were recorded. The maximum depth of indentation and the unloading curve were used to calculate the reduced modulus of the composite. The

reduced modulus of the PLLA/MWCNT films was derived from the unloading portion of the loading displacement curve on an indent following the procedures of Oliver and Pharr (Oliver et. al, 1992).

3.4. Cellular response characterisation

3.4.1. Cell viability test

The HOB cell was cultured on sterile PLLA/MWCNT film in a 12-well plate. Culture medium was removed. Each film was washed with 2ml 1x cfPBS twice. Then the film was transferred into a new 12-well plate. The cell was detached by 0.5mL of trypsin/EDTA and 0.5ml PBS at 37^{o}C for 10 minutes. The film was removed and the suspension was pipetted into a 15ml centrifuge tube and centrifuged at 2000rpm for 5 minutes. The supernatant was discarded. The cells were re-suspensed by vortexing with 2 ml fresh culture medium. Each suspension was transferred into a 4ml cup and placed into a cytometer (Vi-CELL XR Cell Viability Analyzer, Beckman Coulter, USA). CHO cell profile was selected. The cell suspension was divided into 50 portions and 50 pictures were taken after stained by Trypan Blue dye (15250-061, Invitrogen Corporation). The number of living cell and dead cell were counted.

3.4.2. Cell metabolism assay

3-[4,5-dimethyl-thiazol-2-yl]-2,5-diphenyltetrazolium bromide (MTT) powder was dissolved in sterile 1x cfPBS at 5mg/ml. The solution was filtered by 0.22 μm PES membrane (Millipore) in a UV-radiated biological safety cabinet. The stock solution was kept in brown bottle and was sealed by parafilm. The filtered solution was stored at 4 ^{o}C. HOB cell cultured on six different PLLA/MWCNT film at different days in 12-well plate was arranged. Culture medium was removed. Each film was washed with 2ml

1x cfPBS twice. Then the film was transferred into a new 12-well plate. The cells on each film were detached by 0.5mL of trypsin/EDTA and 0.5ml cfPBS at 37^{o}C for 10 minutes. The film was removed and the suspension was pipetted into a 15ml centrifuge tube and centrifuged at 2000rpm for 5 minutes. The supernatant was discarded. The cells were re-suspensed by vortexing with 2 ml fresh phenol red-free culture medium to give total six cell suspension for each different day. Each cell suspension was serially-diluted to give 4 different concentrations. 160µl of each cell suspension was added into the wells of a 96 well plate. A control well was prepared by adding phenol red-free medium without cell. Then 10µl of 5mg/ml MTT solution was added into each well. The plate was incubated at 37^{o}C for 4 hours sealed by aluminium foil. 100µl of DMSO was added into each well to dissolve the formazan salt. Then the plate was placed on a shaker at for 1-minute orbital shaking. The lid was removed and absorbance will be determined at 570nm by a microplate reader (Infinite F200 series, Tecan, Switzerland).

3.4.3. Alkaline phosphatase activity

A sterile centrifuge tube was prepared by adding a tablet of P-nitrophenyl phosphate tablet (pNPP) (N1891, Sigma-Aldrich, USA) into 5ml of PBS solution in (1.0 mg/ml). Another sterile centrifuge tube was prepared by adding a pill of Tris/MgCl (N1891, Sigma-Aldrich, USA) to yield 0.2M Tris Buffer and 5mM MgCl. They were sealed by parafilm and kept at 4^{o}C. Cell suspension cultured at different film at different days was prepared.

The HOB cell cultured on six different PLLA/MWCNT film at different days in 12-well plate was arranged. Culture medium was removed. Each film was washed with 2ml 1x cfPBS twice. Then the film was transferred into a new 12-well plate. The cells on each film were detached by 0.5mL of trypsin/EDTA and 0.5ml PBS at 37^{o}C for 10

minutes. The film was removed and the suspension was pipetted into a 15ml centrifuge tube and centrifuged at 2000rpm for 5 minutes. The supernatant was discarded. The cells were re-suspensed by vortexing with 2 ml fresh phenol red-free culture medium to give total six cell suspension for each different day. Each cell suspension was serially-diluted to give 4 different concentrations. 160µl of each cell suspension was added into the wells of a 96 well plate. A control well was prepared by adding phenol red-free medium without cell. 10µl of 1% Triton-X 100/PBS solution was added to each well to permeabilize the cells. Then 50µl of pNPP and 50µl of Tris/MgCl solution was added into each well. The plate was incubated at 37 ^{o}C for 30 minutes sealed by aluminium foil. 25µl of 3M NaOH solution was added to stop the reaction. Then the plate was placed on a shaker at for 1-minute orbital shaking. The lid was removed and absorbance will be determined at 405nm by a microplate reader (Infinite F200 series, Tecan, Switzerland).

3.4.4. Cytoskeleton morphology and Focal adhesion staining

A sample was placed on a microscopic slide. 4% paraformaldehyde/1xPBS was added to fix the cells for 15 minutes. Wash buffer (0.05% Tween-20 in 1x PBS) was prepared to wash the sample for three times. Permeabilising buffer (0.1% Triton X-100 in 1xPBS) was added at room temperature for 5 minutes. 1% BSA in 1xPBS was prepared as blocking solution and was added to dilute monoclonal anti-vinculin monoclonal antibody (90227, Chemicon) from 1mg/ml to 10µg/ml. 50µl of diluted antibody solution was added into sample. Incubation was followed at 37 ^{o}C for 60 minutes. Wash buffer was used to wash the sample three times at 5 minutes interval. Phalloidin-Tetramethylrhodamine B isothiocyanate (P1951, Sigma-Aldrich, USA), dissolved in methanol to give 0.05mg/ml solution and FITC-conjugated secondary antibody (AP124F, Chemicon), were added into the sample and incubated at 37 ^{o}C for 1

hour. The sample was washed by wash buffer three times at 5 minutes interval. 10µl of DAPI (90229, Chemicon) was diluted to 500µl by Tris buffer. 200µl of diluted DAPI was added to each sample. After 5 minutes incubation, the sample was washed by wash buffer three times at 5 minutes interval. 100µl of 4% N-propyl gallate (1212419, ILUSA) in 90/10 glycerol/PBS was added as mountant. A coverslip was used to cover the sample surface. Confocal laser scanning microscope (Carl Zeiss) and Nikon Eclipse 80i fluorescent microscope was used to observe the fluorescent image at 488nm and 543nm excitation, 550nm and 560nm emission.

Chapter 4: Result

4.1. Biomaterial characterisation

4.1.1. PLLA/MWCNT film fabricated by solvent casting method

PLLA composite with different ratio of MWCNT were successfully fabricated by the methods described in methodology section (Figure 4-1). It could be observed that there was a gradual increase in degree of blackness from control to PLLA with 6.25% of MWCNT. Uniform surface with randomly distributed MWCNT was observed.

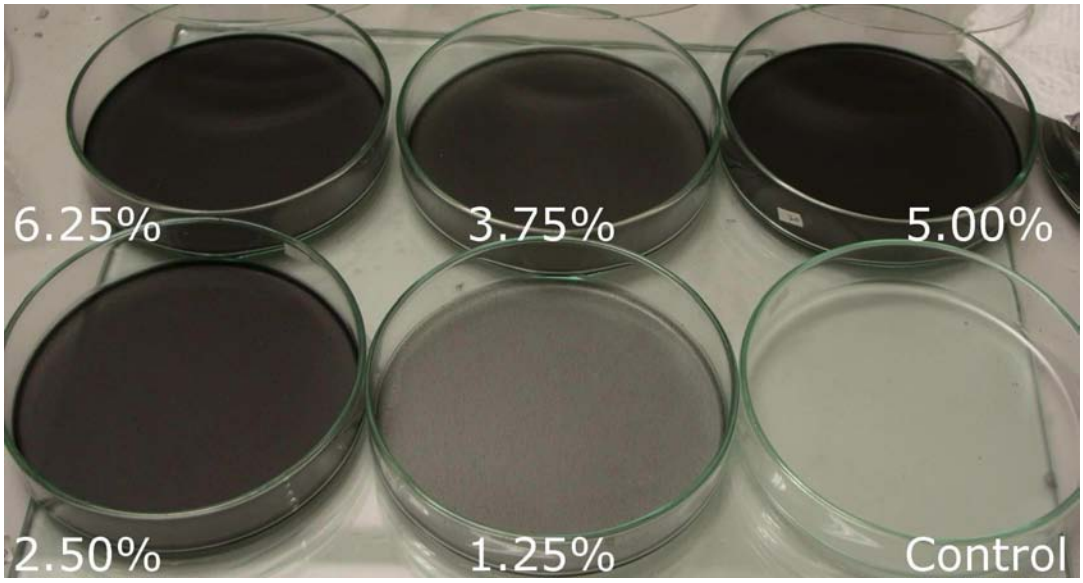

Figure 4-1 Fabrication of Solvent-casted PLLA composite with different amount of MWCNT

4.1.2. Scanning Electron Microscopy

Scanning Electron Microscopy analysis was performed in order to investigate the surface property and the dispersion homogeneity of MWCNT in the polymeric matrix. The surface of the film without carbon nanotubes was very smooth and free of defects (Figure not shown). For PLLA incorporated with different amount of MWCNT, exposed MWCNT could be observed on the surface. The SEM images showed that coatings were uniformly thick and appeared microstructrally homogeneous at 10,000x magnification (Figure 4-2). It clearly indicated the presence of MWCNTs on the surface

of the composite as well as embedded inside the polymer matrix. The tubular structure of MWCNT was preserved and did not have visible damages or shortening. The orientation of MWCNT seemed to be random. No distinct alignment and orientation of MWCNT could be found. Generally, PLLA composite with higher amount of MWCNT showed a higher amount of randomly exposed MWCNT and longer exposed bundle (Figure 4-2). It also represented a higher degree of surface roughness. It must be mentioned that surface roughness may be helpful for the growth of cells because this property can influence the protein interaction leading which is involved in cell adhesion.

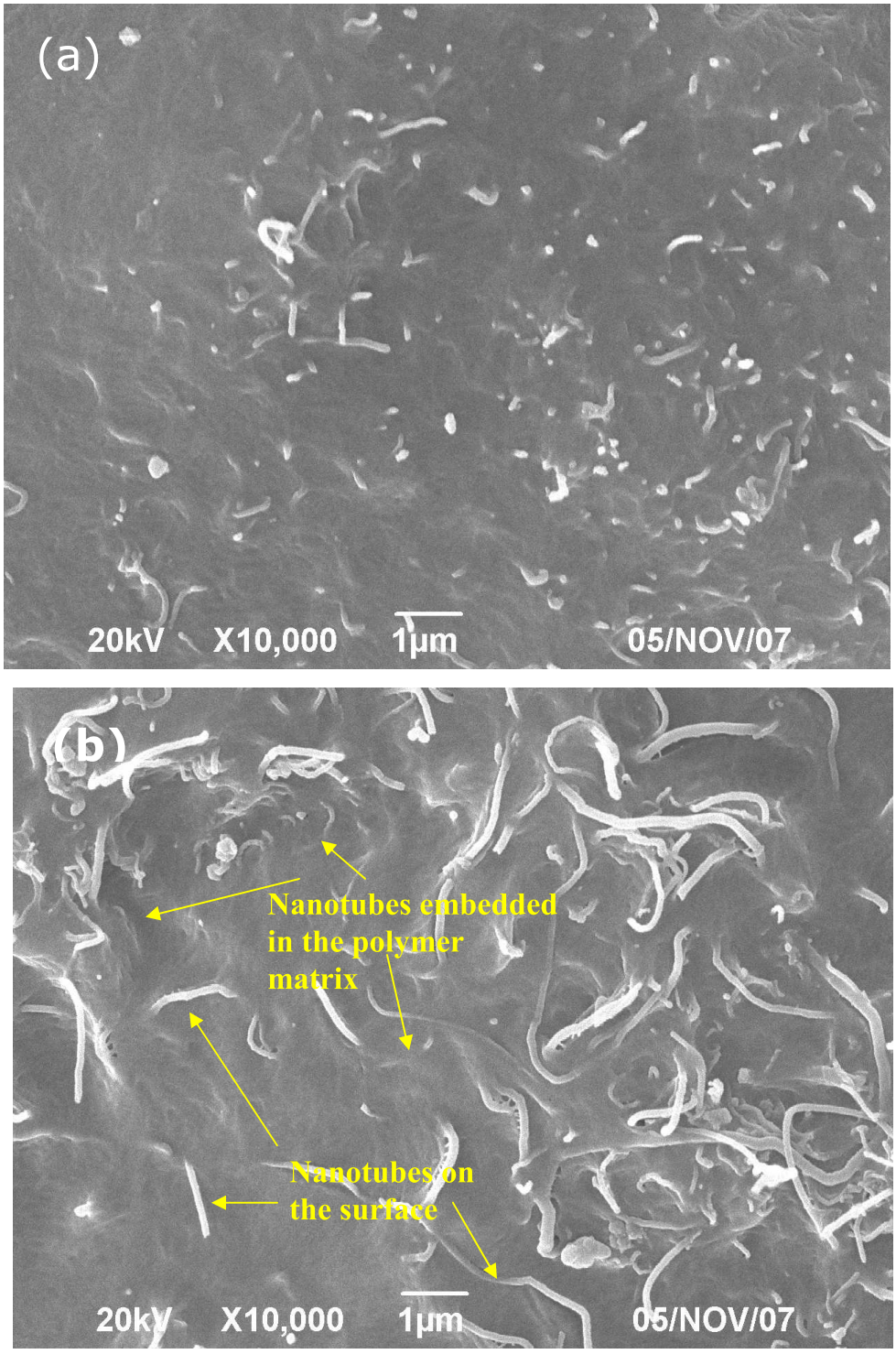

Figure 4-2 SEM pictures of a) PLLA/3.75% MWCNT and b) PLLA/6.25% composite

4.1.3. Energy Dispersive X-ray Spectrometry

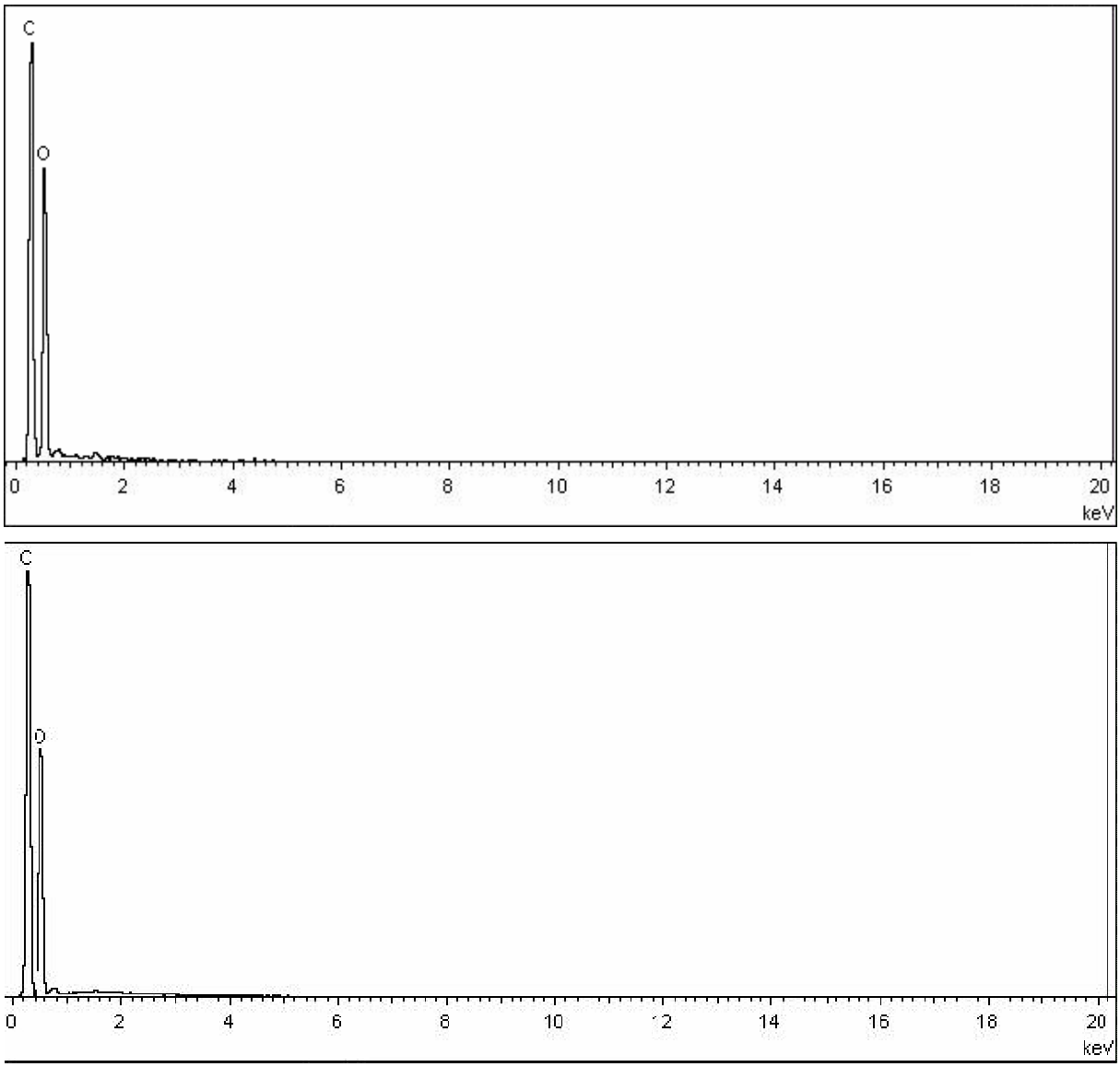

Figure 4-3 An EDX Spectrum of pure PLLA (Top) and PLLA with 6.25% MWCNT (Bottom)

Spot analysis via Energy Dispersive X-ray Spectroscopy (EDX) was shown in Figure 4-3. Two distinguished peaks, which represent the relative content of carbon and oxygen in PLLA and MWCNT, could be observed from the spectrum. The obvious increasing of carbon to oxygen ratio (C/O ratio) was observed from PLLA control to PLLA/6.25% MWCNT composite. In the fabrication process, chloroform was used in sample fabrication. The content of chlorine element was also analysed to determine the

amount of remaining content (Figure 4-4). Less than 0.01% of chlorine was detected for all samples. This showed that nearly no chloroform used in sample fabrication was remained in the sample or reacted with the samples chemically.

Table 4-1 The carbon to oxygen ratio of PLLA/MWCNT composite

	0%	*1.25%*	*2.5%*	*3.75%*	*5%*	*6.25%*
Theoretical C/O Ratio	1.1250	1.1535	1.1827	1.2127	1.2434	1.2750
Detected C/O Ratio (Normalized average)	1.1250	1.1533	1.1872	1.2114	1.2631	1.2731
Detected C/O Ratio (SD)	0.0312	0.0322	0.0194	0.0240	0.0307	0.0163

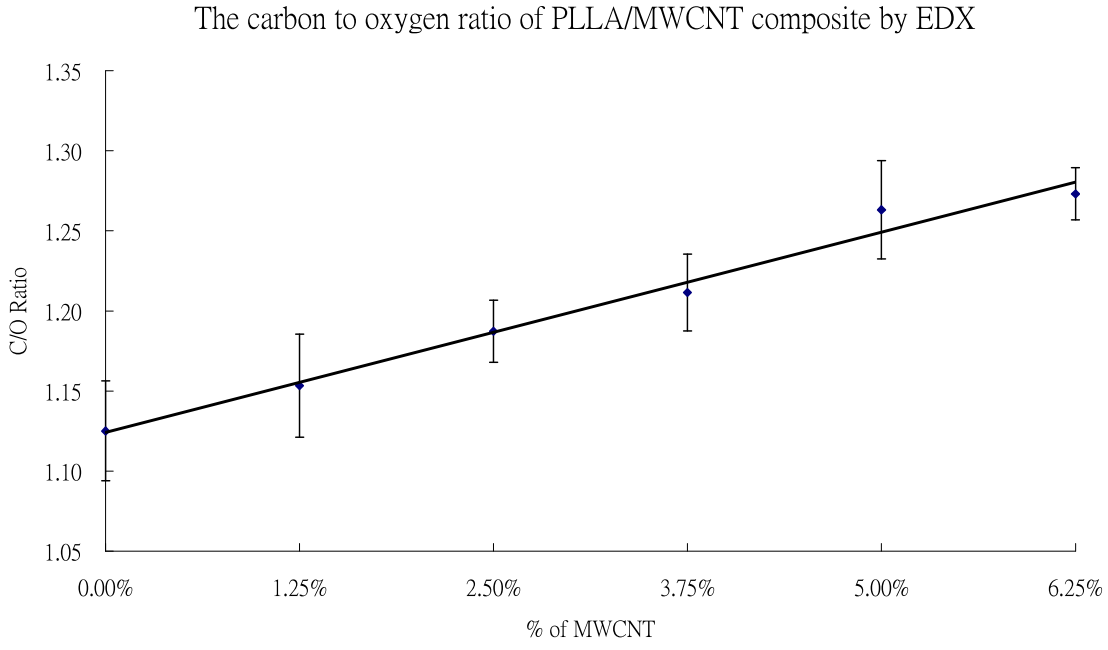

Figure 4-4 Carbon to oxygen ratio of PLLA/MWCNT composite by EDX

The theoretical analysis and corresponding EDX results for different PLLA/MWCNT composite were showed in Table 4-1. The gradual increase of carbon content of PLLA/MWCNT composite was due to the increased loading of MWCNT. It

was believed that the ratio increase was contributed by the addition of MWCNT since the carbon content of MWCNT is higher than PLLA. For sample with no MWCNT, the theoretical ratio is 1.125. For composite with different amount of MWCNT added, the calculated C/O ratio was slightly different from the detected C/O ratio. When 1.25% of MWCNT was added into the sample, the C/O ratio detected by EDX was 1.1533, which is 0.0173 smaller than the calculated ratio. For PLLA/2.50% MWCNT composite, 1.1867 C/O ratio was detected. It is 0.4% higher than the calculated ratio. This also occurs for PLLA/5.00% MWCNT composite, which had a 1.58% higher C/O ratio than the calculated ratio. For PLLA/3.75% and PLLA/6.25% MWCNT, a slightly lower C/O ratio was detected.

4.1.4. X-ray Diffraction Spectrometry

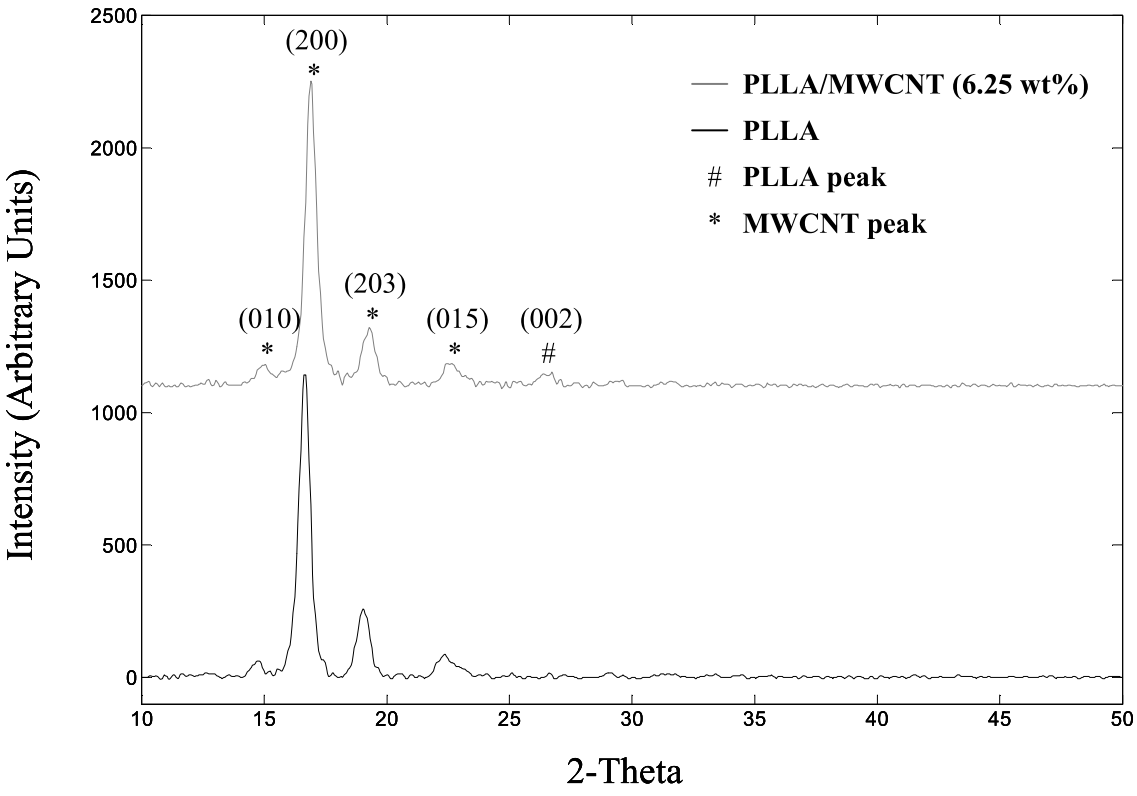

Figure 4-5 XRD Spectrum of PLLA control (Top) and PLLA/6.25% MWCNT samples (Bottom)

The X-ray diffraction spectrum was measured from 10 degree to 50 degree to identify and observe the crystallinity of the PLLA samples incorporated with different amount of MWCNT. The spectrum showed very sharp PLLA crystalline peaks at 2θ angle of 14.8 degree, 16.8 degree, 19.4 degree and 22.5 degree for all samples (Figure 4-5). When the amount of incorporated MWCNT increased, a crystalline peak at 26 degree for MWCNT became more observable for samples with 6.25% MWCNT. This confirmed that MWCNT had been successfully incorporated into PLLA film. In the spectrum, absence of other peaks indicated that the incorporation of MWCNT and the use of chloroform solvent didn't affect the physical structure of PLLA samples. It also confirmed that no degradation or other chemical reaction during the fabrication process. Similar degree of crystallinity was also observed for all PLLA/MWCNT samples according to the peak height. However, the peaks for sample with less than 5% MWCNT were too minute to be detected in the spectrum.

4.1.5. Nanoindentation

Table 4-2 Mechanical properties of PLLA/MWCNT composite characterised by nanoindentation

% MWCNT	*0.00%*	*1.25%*	*2.50%*	*3.75%*	*5.00%*	*6.25%*
Young's Modulus (GPa)	3.6	4.4	5.8	6.6	7.5	7.8
Relative Young's Modulus to Control Ratio	1.00	1.22	1.61	1.83	2.08	2.17
% increase in Young's modulus/% MWCNT		17.60	24.40	22.13	21.60	18.72

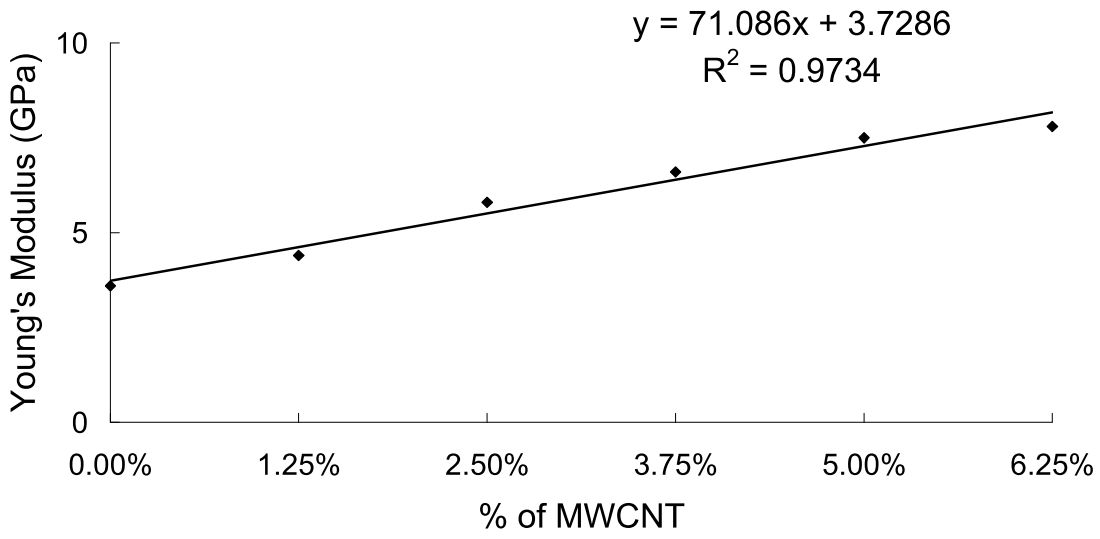

Figure 4-6 Nanoindentation result of PLLA/MWCNT samples

The result of nanoindentation showed that the increasing of carbon nanotube content enhanced the modulus of composite. A gradual increasing of modulus could be observed with the continuous addition of MWCNT. This indicated that MWCNT was a very effective material to strengthen PLLA samples. Only a few percentage of MWCNT could substantially increase the modulus of PLLA film. For samples with 6.25% of MWCNT, the net gain in mechanical strength decreases to 8%, which was lower than 22%, 39%, 22% and 35% increases of prior samples. It might suggest that the reinforcement effect would lower down when the MWCNT content within polymeric matrix continuously increases.

4.2. Cellular Response Characterisation

4.2.1. SEM characterization of HOB cell cultured on PLLA/MWCNT film

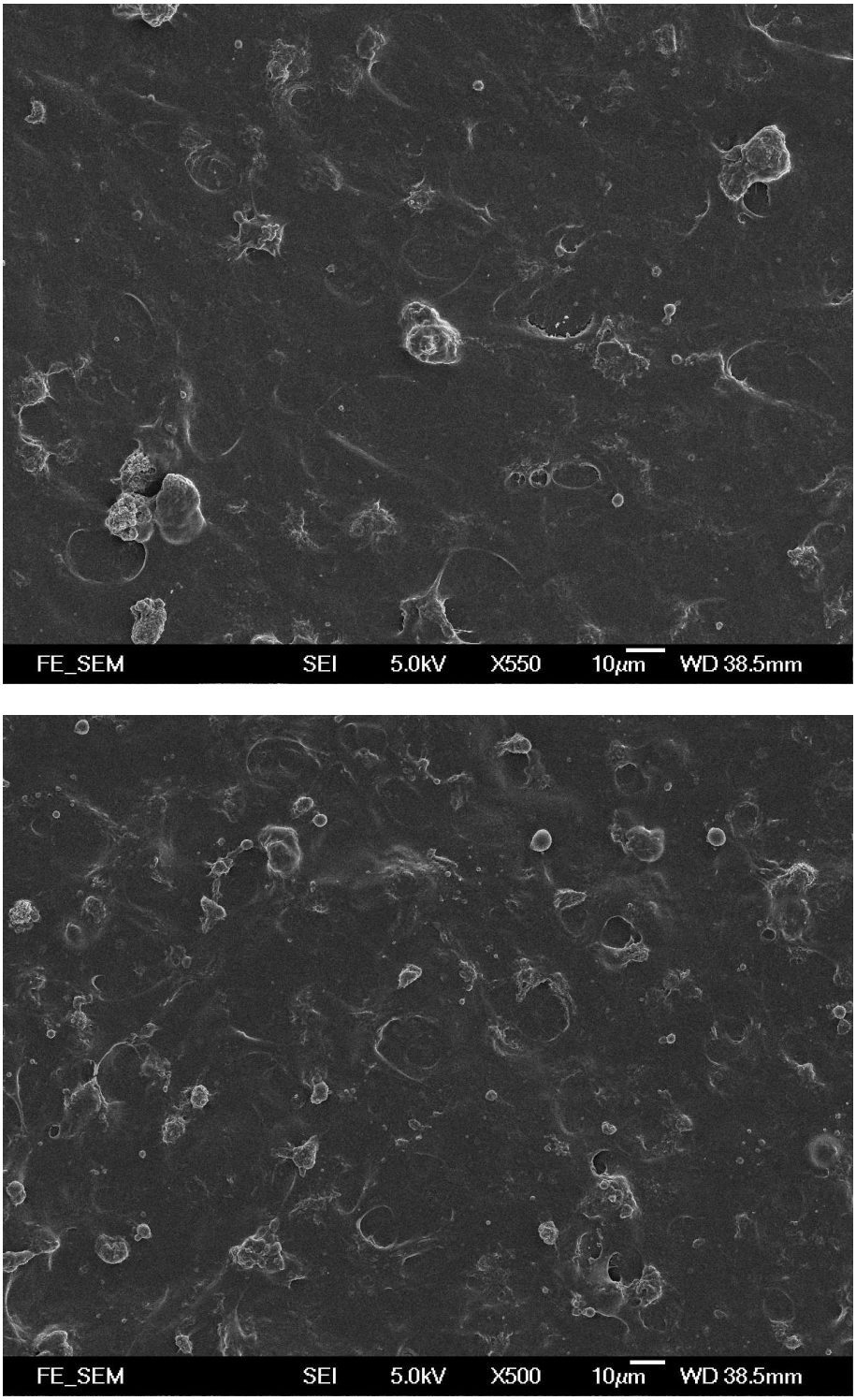

Figure 4-7 SEM picture of HOB cell cultured on a) PLLA sample and b) PLLA/6.25% MWCNT composite after 5 days

The cell morphology and attachment of PLLA and PLLA/MWCNT composite film were observed using SEM as shown in Figure 4-7. As shown in Figure 4-7, a lot of HOB cell was found attached on the surface of the PLLA sample (Fig 4-7a) and PLLA/6.25% MWCNT composite (Fig 4-7b) after 5 days culture. There were no

observable differences in morphology of HOB cell between different samples. The HOB cells were randomly distributed and did not exhibit special orientation. High magnification pictures had been taken and shown in figure 4.8. Again, it was difficult to distinguish if the HOB cell had any morphological differences.

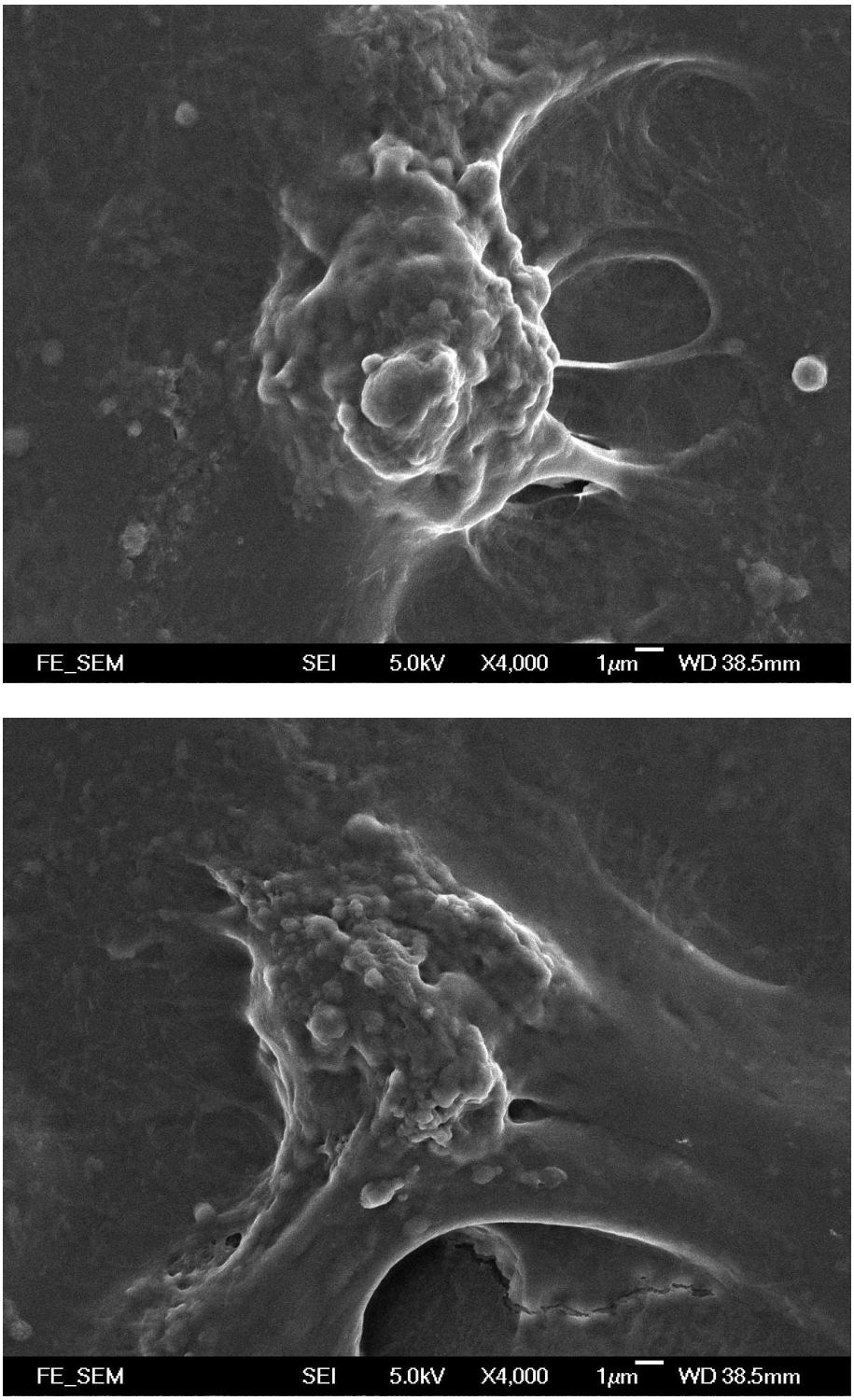

Figure 4-8 SEM picture of HOB cell cultured on a) PLLA sample and b) PLLA/6.25% MWCNT composite after 5 days in 4000x magnification.

4.2.2. Cytoskeleton morphology

Figure 4.9 showed the fluorescent image of HOB cell cultured on PLLA and PLLA/6.25% MWCNT composite. The actin cytoskeleton of HOB cell was stained with phalloidin-Tetramethylrhodamine B isothiocyanate (Red) and cell nucleus was stained with DAPI (Blue) (Figure 4.9). Large number of attached cells could be observed on PLLA sample and PLLA/MWCNT composite. These showed that the surface of composite film provided a good and non-toxic environment for cells to undergo active proliferation and spreading. From the picture, it seemed that more cells were grown on PLLA/MWCNT composite than PLLA control sample. It suggested that the PLLA/MWCNT composite provided some advantages over the control sample for cell growth. In Figure 4-10, the morphology of the stained actin cytoskeleton was clear and highly stressed. It provided a good explanation that the cell had been successfully adhered on the surface. It seemed that both PLLA and PLLA/MWCNT composite provided a good environment for the culturing of HOB cell.

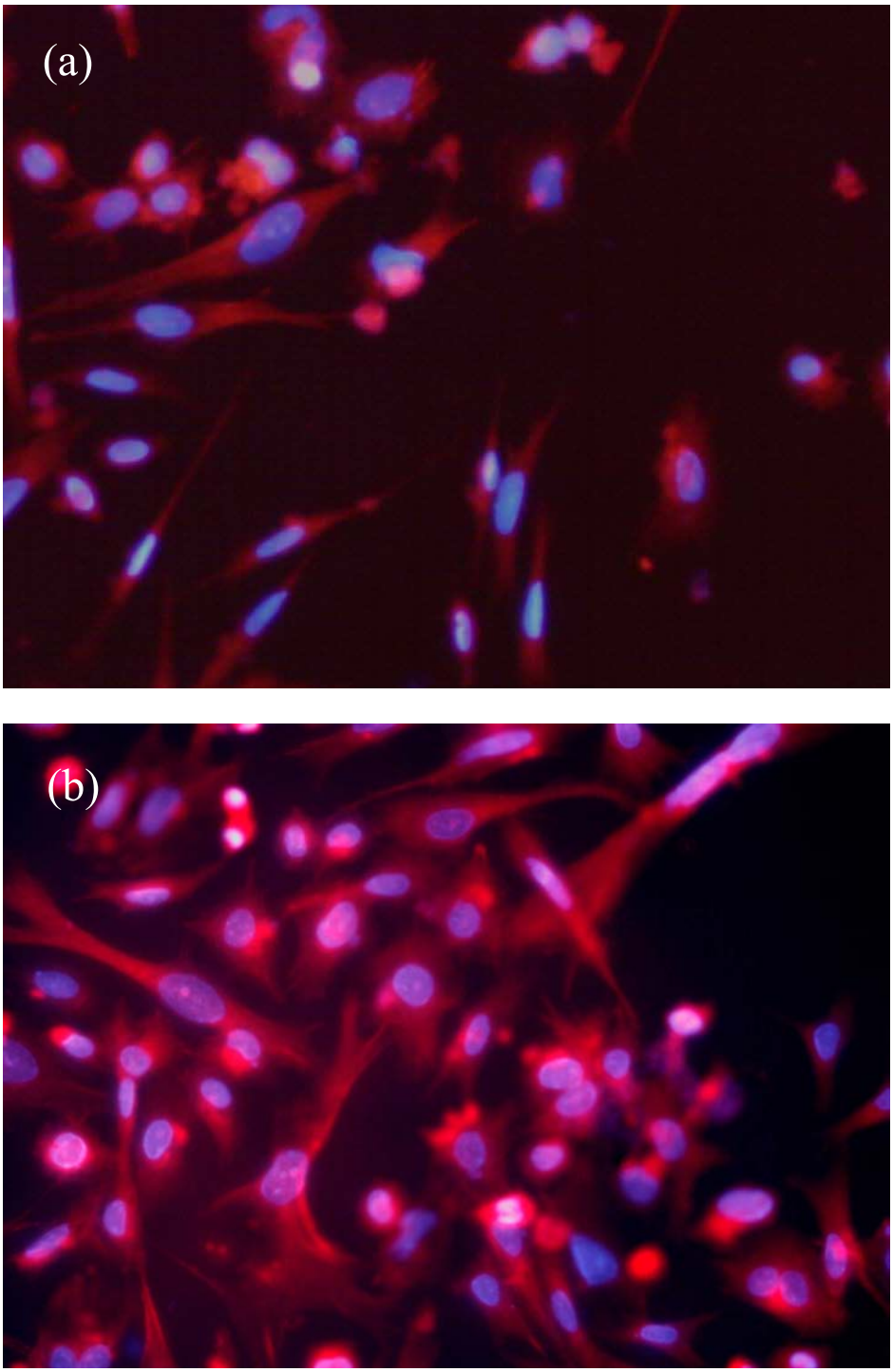

Figure 4-9 Cytoskeleton morphology of cell culture on a) control sample and b) PLLA with 6.25% MWCNT stained with phalloidin-TRITC and DAPI.

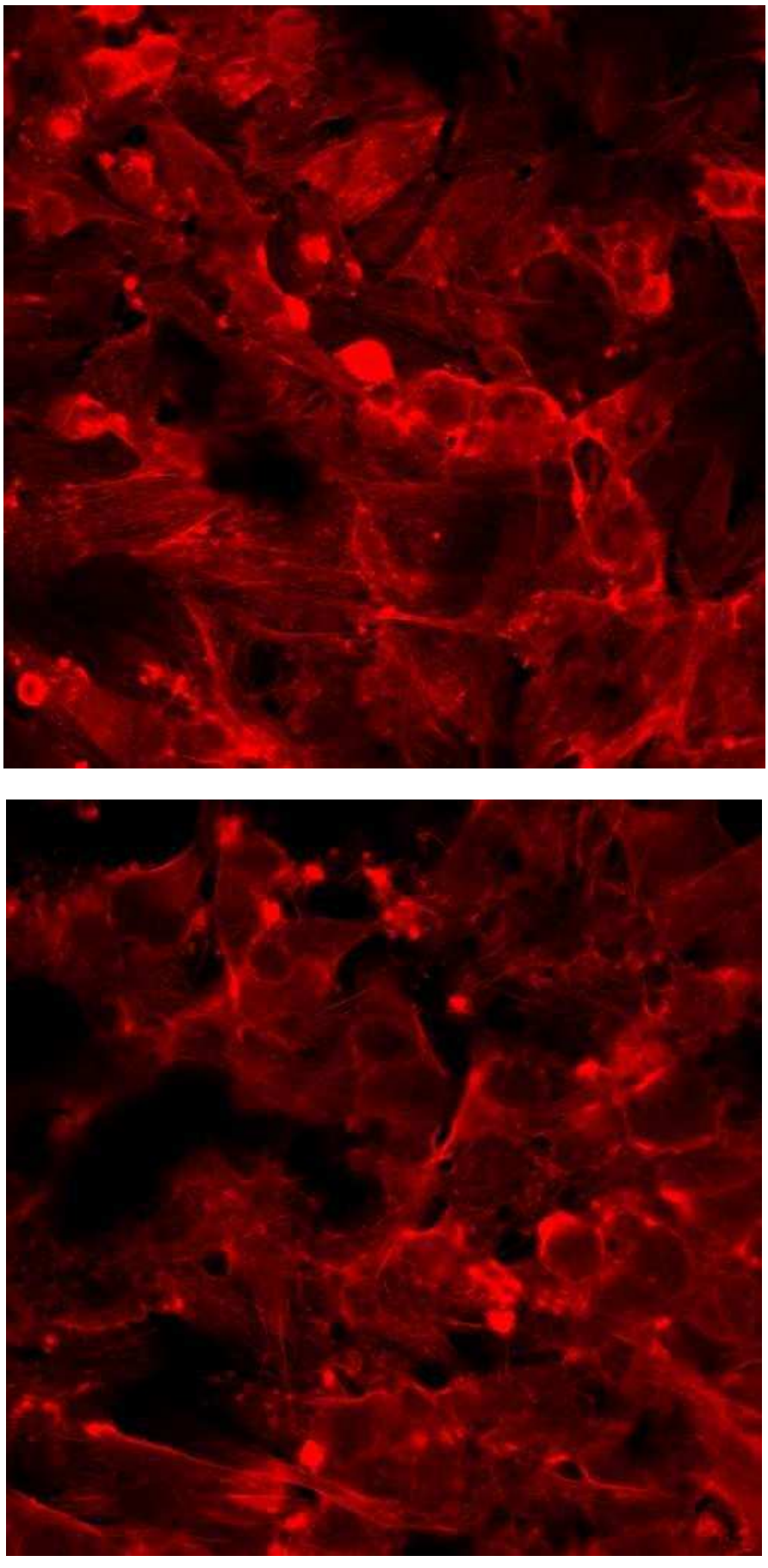

Figure 4-10 Cytoskeleton morphology of cell culture on a) control sample and b) PLLA with 6.25% MWCNT stained with phalloidin-TRITC.

4.2.3. Cell viability test

Table 4-3 Percentage of viable cell after culturing for 2, 4, 6 and 8 days on different composite.

Sample	*2 days*	*4 days*	*6 days*	*8 days*
0%	95% ± 2.63%	94% ± 5.94%	93% ± 2.82%	93% ± 3.22%
1.25%	92% ± 4.77%	92% ± 3.46%	92% ± 2.44%	93% ± 4.37%
2.5%	93% ± 4.35%	91% ± 4.83%	94% ± 4.91%	93% ± 4.02%
3.75%	94% ± 3.19%	93% ± 5.52%	96% ± 2.31%	94% ± 1.44%
5%	97% ± 3.96%	94% ± 4.7%	93% ± 5.5%	95% ± 5.22%
6.25%	95% ± 4.9%	95% ± 5.47%	93% ± 2.97%	96% ± 1.15%
One-way ANOVA p-value	0.444	0.837	0.537	0.793

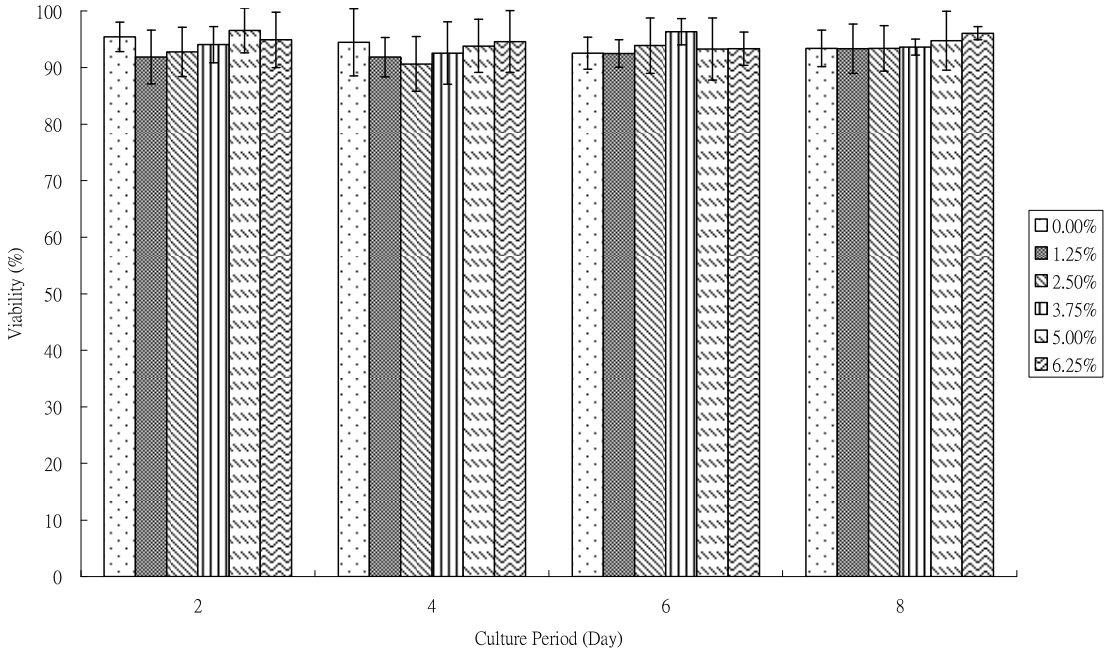

Figure 4-11 Percentage of viable cell after culturing for 2, 4, 6 and 8 days on different composite.

HOB cell had been successfully cultured on the PLLA film with different ratio of MWCNT. Cell viability test had been carried out to test for the cytotoxic effect of

PLLA/MWCNT on HOB. When comparing the viability between the cells cultured on PLLA film and PLLA/MWCNT film, we could see that all cell has viability more than 90%. Statistically, no significant differences were observed for MWCNT content ($p>0.05$). It showed that different amount of MWCNT in PLLA composite has no significant effects on the viability of cell.

4.2.4. Cell metabolism assay

Table 4-4 Relative activity of mitochondrial dehydrogenase of cell after culturing for 2, 4, 6 and 8 days on different composite.

Sample	*2 days*	*4 days*	*6 days*	*8 days*
0%	1.00±0.22	1.00±0.06	1.00±0.41	1.00±0.12
1.25%	1.59±0.31	1.28±0.11	1.30±0.29	1.16±0.22
2.5%	1.52±0.16	1.38±0.26	1.94±0.40	1.55±0.21
3.75%	1.83±0.28	1.81±0.05	2.08±0.26	2.07±0.07
5%	2.19±0.15	1.88±0.08	2.59±0.18	1.96±0.04
6.25%	2.04±0.28	2.25±0.29	2.35±0.15	2.19±0.07
One-way ANOVA p-value	0.027	0.011	0.023	0.002

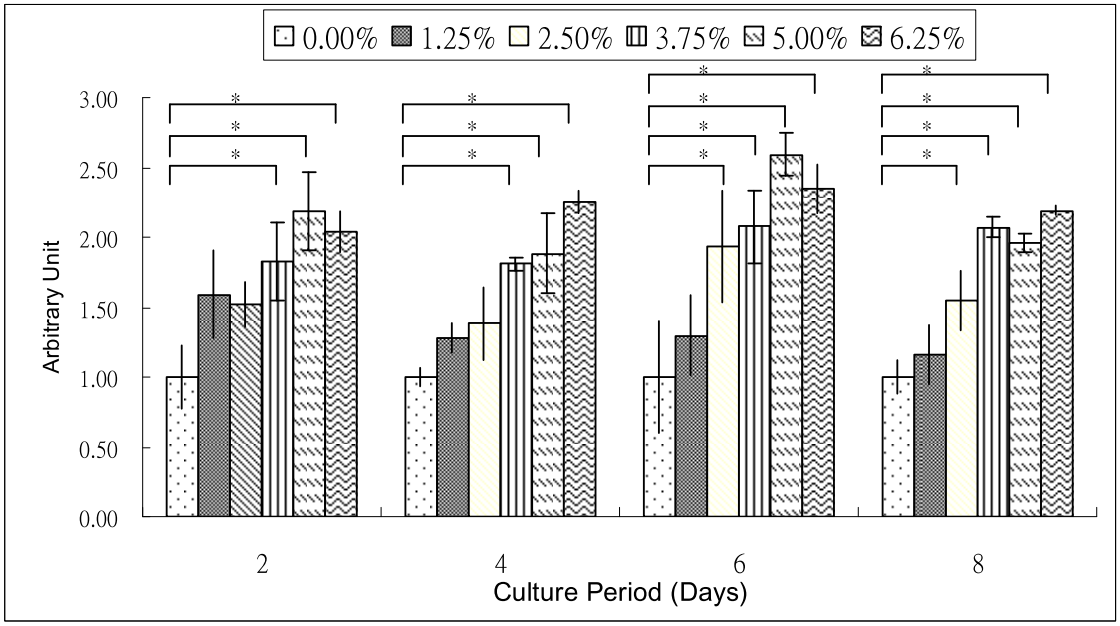

Figure 4-12 Relative activity of mitochondrial dehydrogenase of cell after culturing for 2, 4, 6 and 8 days on different composite. Only data with significant difference from control are shown (* $p<0.05$).

Figure 4-12 shows the relative activity of mitochondrial dehydrogenase (MD) of cell. After two days culturing, we could see that the activities of MD cultured on all PLLA/MWCNT composites were higher than the control. The activity of MD increased when MWCNT content increased. It reached the highest for PLLA/5% MWCNT composite. The activity of MD was slightly lower for PLLA/6.25% MWCNT composite. At the forth culturing days, the control got the lowest activity of MD enzyme. PLLA/5% MWCNT composite had the highest MD activity than the others. At the sixth day, PLLA/6.25% MWCNT composite had the highest MD activity. Control had the lowest MD activity. After eight days culturing, PLLA/3.75% and PLLA/6.25% MWCNT composite had the highest activity. The activity of MD of the control was lowest. After these eight days culturing and monitoring, we found that the addition of MWCNT to PLLA did not cause any decrease in activity of MD. All cell cultured on PLLA/MWCNT composites had higher activity of MD than control. This might due to the increase in mechanical strength of composite. We also found that the activity of MD

was the highest if the MWCNT ratio exceeds 3.75%, it showed that MWCNT exceeds this ratio could give the highest MD activity among the other samples. The results of One-way ANOVA test showed that there were significant differences between samples in all sample groups ($p<0.05$). LSD Multiple comparison showed that the MD activity of cell cultured on PLLA/6.25% MWCNT and PLLA/5.00% MWCNT composite was significantly different from the control for all four different culturing period ($p<0.05$).

4.2.5. Alkaline phosphatase activity

Table 4-5 Relative activity of alkaline phosphatase of cell after culturing for 2, 4, 6 and 8 days on different composite.

Sample	*2 days*	*4 days*	*6 days*	*8 days*
0%	1.00±0.14	1.00±0.74	1.00±0.36	1.00±0.10
1.25%	1.62±0.60	1.28±0.53	1.71±0.71	1.38±0.06
2.5%	1.72±0.51	1.60±0.67	1.40±1.03	1.69±0.12
3.75%	2.16±0.26	1.67±0.78	1.88±0.57	1.55±0.06
5%	2.44±0.01	2.12±0.57	2.37±0.69	1.75±0.47
6.25%	2.03±0.16	2.14±0.12	2.32±1.22	1.47±0.18
One-way ANOVA p-value	0.341	0.725	0.953	0.459

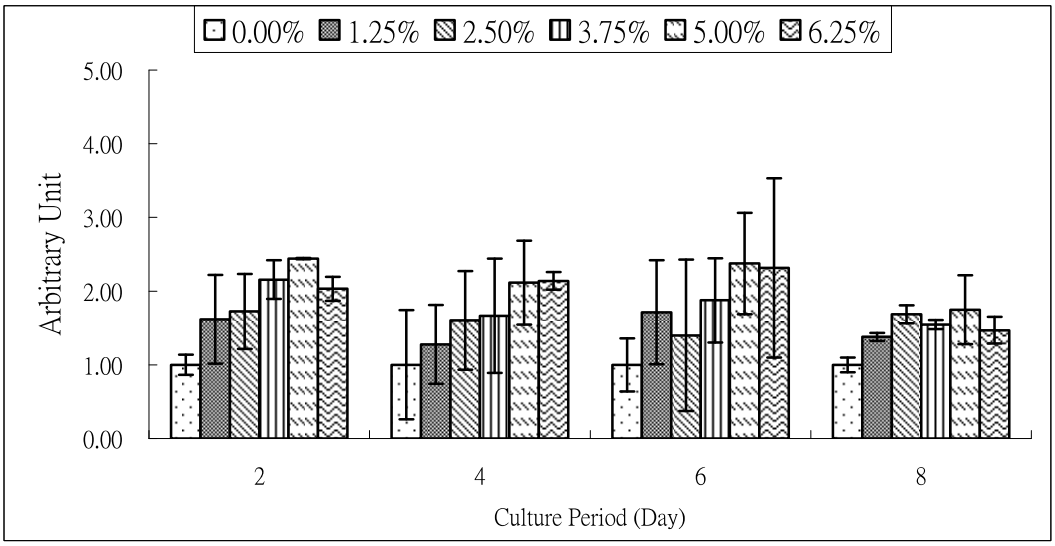

Figure 4-13 Relative activity of alkaline phosphatase of cell after culturing for 2, 4, 6 and 8 days on different composite. Data of each day was analysed by one-way ANOVA.

Figure 4-13 showed that the activity of alkaline phosphatase (ALP) enzyme in cell cultured on PLLA or PLLA/MWCNT composite. After two days culture, we could observe that the ALP activity is the highest for PLLA/5.00% MWCNT composite, which was coincide with the cell metabolism assay. The control had the lowest ALP activity. The same observation occurred at the forth culturing day, at which PLLA/6.25% MWCNT composite had the highest MD and ALP activity. The control had the lowest ALP activity again. At the sixth day, the activity of ALP of cell cultured on PLLA/5.00% composite was the highest. After eight days culture, cell cultured on PLLA/5.00% MWCNT composite had the highest ALP activity. It seemed that PLLA sample with 3.75% or above MWCNT could give the most effective simulate to the activity of ALP enzyme. The result of One-way ANOVA showed that there was no significant difference between samples in each culture period ($p<0.05$).

Chapter 5: Discussion

5.1. PLLA/MWCNT Composite Characterisation

Since MWCNT has strong van der Waal's interaction, strong anisotropic interaction and a high length to diameter ratio, they would easily aggregate into tangled networks. The purchased MWCNT was highly entangled and form big bundles up to 5mm. They formed stable aggregations inside organic solvent even after shaking. To disperse the entangled MWCNT network, the method reported by Li Q et al. (2005) had been evaluated. After the addition of MWCNT into NaOH in 80% ethanol solution and ultrasonicated for 600 minutes in the ultrasonic bath, a lot of carbon nanotubes were still entangled and visible in the liquid. Filtration with 0.45 μm PES membrane had been carried out to see if dispersed MWCNT can be obtained. Most of the MWCNT was cogged inside the filter membrane. The filtrate contain minute of MWCNT and became entangled again after the removal of NaOH-ethanol solvent. The standalone sonication method had also been used. Two low power ultrasound water bath (35W@42kHz and 50W@42kHz) and one high power ultrasound transducer has been compared (400W@24kHz). The low power ultrasound transducer had been found ineffective, after ultrasonication with a 40W ultrasound water bath for 600 minutes, large bundle of MWCNT was still observable by naked eye in chloroform solvent. When the mixture was settled for 5 minutes, large bundles of MWCNT sank to the bottom of the tube. There was no visible difference before and after ultrasonication. The high power ultrasound transducer was much effective. A ten seconds ultrasonication resulted in thoroughly distributed MWCNT in chloroform solvent. The resultant solution was stable and has no observable re-entanglement after one week. There were some controversies between results of dispersion of MWCNT done by Li Q et al. (2005). The reason may due to the differences in samples. Li Q et al (2005) use SWCNT, which was

different from MWCNT was used in our experiment. The power of the ultrasonic bath and diameter and length of SWCNT used by Li Q et al (2005) was not reported. These were very important as the degree of aggregation is partially depends on the length to diameter ratio of CNT. The power of the ultrasonic bath could also change the time required for effective CNT dispersion. Comparatively, the energy of ultrasound transducer seems to govern the effectiveness of CNT dispersion in chloroform solvent. High energy could disperse MWCNT just within a few seconds. MWCNT in deionized water has also been sonicated to evaluate if different solvent can resulted in different result. After 10 seconds of high power ultrasonication, MWCNT in deionized water also was able to form a thoroughly distributed MWCNT in solution. Therefore, a standalone ultrasonication with high power is enough to disperse the MWCNT, without the additional of other solvent and dispersing agent. It may also be applicable in SWCNT and other functionalized CNT.

The reason of higher power ultrasound to give better dispersing result can be understood as followings. When ultrasound is generated by the ultrasound transducer, the energy of ultrasound wave is absorbed and causes the collapsing or creation of cavitations bubbles. These bubbles can loosen and unwind the entangled MWCNT. Higher energy can generate higher energy shock wave and having higher unwinding power. CNT has strong covalent bonded carbon and be able to withstand higher power. Therefore, the use of high energy ultrasonic wave can produce better efficiency of MWCNT dispersion.

From the pictures taken by SEM, it showed that some protruded MWCNT was distributed on the PLLA surface. Its tubular structure was intact and doesn’t have any visual damages and shortening. It showed that MWCNT has been successfully

incorporated into the PLLA film. From the pictures, some dull tubular structures were observed from the film surface, especially in figure 4.2b. They were expected to be the embedded MWCNT. They did not have bright white colour because of the charging up of MWCNT on surface but not MWCNT embedded inside the composite. The integrity of MWCNT was further confirmed by EDX and XRD characterization.

From the XRD spectrum, we could observe a MWCNT peak for sample with 6.75% MWCNT. It showed that MWCNT was successfully incorporated into PLLA film. However, the MWCNT peak for sample with lower MWCNT is not quite visible. The reason behind may be the limited sensitivity of XRD to material with low concentration. Moreover, the content of MWCNT is quite limited when comparing with PLLA, the MWCNT to PLLA ratio ranged from 1:79 to 1:15, the XRD count for PLLA peak should be higher than MWCNT content and may be masked out the MWCNT peak. Furthermore, XRD monitors the x-ray scattered from the crystalline material, PLLA is a crystalline material and is more detectable than nearly non-crystalline MWCNT. This can create a big difference between the peak count of PLLA and MWCNT. Actually, reducing the precision of detection angle and increasing the counting time may increase the peak, however, 0.001 degree angle increment and 8 seconds per count has been tried but there is no significant improvement for the MWCNT peak.

The EDX spectrum shows an increase of C/O ratio, which represent a higher carbon ratio in the PLLA sample with more MWCNT. This is consistent with our expectation since the additional of MWCNT will increase the carbon ratio to PLLA ratio. In the repeating unit of PLLA polymer, it has three carbon atoms, two oxygen atoms and four hydrogen atoms. Each PLLA repeating unit can be replaced by six carbon atoms. By simple calculation by weight ratio and normalisation, the C/O ratio for

pure PLLA film is expected to be around 1.1250:1. However, when MWCNT is added into the PLLA composite, the increase in C/O ratio is slightly lower than the actual increase of MWCNT content, except for PLLA/5.00% MWCNT composite. These inconsistencies may partially due to the localization of MWCNT. Since MWCNT has strong van der Waal's interaction, strong anisotropic interaction and a high length to diameter ratio, they would easily aggregate into tangled networks. When collecting the EDX spectrum, it is possible that some area with localized MWCNT was selected. This resulted in a higher C/O ratio. This may also create another area with lower calculated C/O ratio. It should be noted that the maximum ratio of inconsistency is 1.58% and is relatively small. The other possibility is that the sensitivity of EDX for different elements may be different. Therefore, slightly variation of the detected C/O ratio is acceptable.

Generally, the PLLA and PLLA/MWCNT composites were brittle at room temperature and thin. Their mechanical properties were difficult to be fully characterized by normal bulk mechanical tests. Nanoindentation provides the possibility of applying extremely light loads and small displacement. The brittleness and thickness were not a critical factor any more. The results of nanoindentation of PLLA/MWCNT composite (Table 4-2), shows a gradual increase in modulus when MWCNT content increases. When MWCNT was added into PLLA continuously, the strong MWCNT would gradually give reinforcement effects to PLLA film (Figure 4-6). The comparison of reduced modulus of the nanotube-reinforced surface with pure PLLA surface indicated that the MWCNT-reinforced PLLA surface was much stiffer since the surface stiffness was proportional to the elastic modulus of the sample. The results show a nearly linear strengthening of surface mechanical property with the linear increasing of MWCNT content within the small amount (<wt 6.25%). With the increasing of

MWCNT content upto 2.50% w/w, the reinforcement effects started to lower down. This phenomenon could be understood as following. When MWCNT was added into PLLA continuously, the strong MWCNT can give reinforcement effects to PLLA film. However, part of the mechanical performance of PLLA/MWCNT composite is contributed by the crystallinity PLLA polymer. When more MWCNT is added, the effect of the reinforcement reduced since MWCNT molecules may hinder the crystallisation of PLLA polymer. This disruption of crystallisation of PLLA polymer contributes to a reduction in overall reinforcement efficiency.

Hydroxyapatite (HA) is a common bioceramics used to reinforce PLLA. From the study carried out by Wright-Charlesworth et al (2006). They measured the modulus of PLLA reinforced by HA as shown in table 5-3. For pure PLLA, it could be observed that the modulus of pure PLLA used in our experiment was slightly weaker than the one used by Wright-Charlesworth et al (2006). However, after addition of 1.25% MWCNT into PLLA, it had the modulus comparable to the 10% HA-PLLA. Addition of 2.5% MWCNT into PLLA resulted in the same modulus to the 30% HA-PLLA. 40% HA-PLLA was comparable to PLLA/3.75% MWCNT only. It showed that MWCNT provided a more efficient reinforcement power than HA.

5.2. Cell Response Characterisation

From the SEM pictures, the surface of PLLA and PLLA/MWCNT composite was covered by many cells. They provided very good evidence that the HOB cell was successfully cultured on PLLA/MWCNT composite. Cell cultured on both sample showed similar overview and suggested that they had no obvious difference in growing pattern. The HOB cell on both samples seemed to be randomly distributed. No

distinguishable orientation or localised proliferation was observed. Morphology of cell had been analysis in picture with high magnification but no distinguishable morphological differences were notice.

From the CLSM pictures, large number of cells was observed from the surface of the PLLA and PLLA/MWCNT composite. It showed that the PLLA/MWCNT composite had good biocompatibility. It allowed good proliferation of the HOB cell. The good proliferation of the cell could be further explained by the clustering and stacking of proliferated cell, which suggest the clustered cells were originated from the same ancestor. Therefore, active cell division occurred on both PLLA and PLLA/MWCNT composite surface. It was consistent to our finding from the SEM pictures. Actin cytoskeleton of cell cultured on PLLA sample and PLLA/MWCNT composite had been clearly stained. Claw-like morphology from the edges of the cells and stressed actin cytoskeleton were important markers to show good adhesion to the biomaterial surface. This is an important characteristic to show that the film provides a favourable environment for the growth of HOB cells. After successful cell adhesion, it allowed the potential expression of the differentiation marker by the cell. All of the results represented a good biocompatibility and bioactivity of the film surface.

From the result of cell viability test, it could be observed that over average 90% of cells cultured on different PLLA/MWCNT composite was viable after 2, 4, 6 and 8 days culture. After one-way ANOVA statistical analysis, there is no significant difference between sample groups on each day ($p<0.05$). Even thought there is no significant difference between other sample groups statistically, from the graph of the result, some interesting tendencies could be observed. For PLLA samples with 1.25% MWCNT, the result of cell viability was either the same as or lower than the control

sample for all culturing period. For PLLA samples with 2.50% of MWCNT, the result of cell viability is mostly the same as or lower than the control sample, except day 6. It seems that the cell viability of PLLA samples with 1.25% and 2.50% of MWCNT is slightly lower than the control, even it was not significant. For PLLA samples with 5.00% and 6.25% of MWCNT, the result of cell viability was either the same as or higher than the control sample. It might suggest that the continuous addition of MWCNT would first reduce the cell viability, and then increase the cell viability. It was contrast to our expectation that the cell viability should keep increasing with further addition of MWCNT. This phenomenon might be explained by the protruded MWCNT and degree of reinforcement. When MWCNT was added, some MWCNT was exposed to the surface. It may be sensed by the cell and hinder the cell attachment to the composite surface. The cell which was unable to have good adhesion to the surface may undergo apoptosis. Further addition of MWCNT gave further increase in mechanical properties of PLLA/MWCNT composite. Since osteoblast-like cell was sensitive to mechanical environment, this reinforcement effect may slowly outweigh the adverse effect brings by the exposed MWCNT and result in increase in cell viability.

From the lecture review, it seemed there were some controversies about the cytotoxic effect of MWCNT. In our experiment, the MWCNT was embedded inside the PLLA polymer, and PLLA polymer was a biodegradable biomaterial with slow degradation kinetics. We expected most of the MWCNT would stay inside the PLLA film, but not flowing around in the medium. Therefore, it had low chances of MWCNT intake by the cell. Furthermore, after consideration of the result from various scientists, I believed that the cytotoxic effect of CNT was dose dependent. Some studies used high dose of CNT and found significant cytotoxic effect and other studies used lower dose of CNT and gave no observable cytotoxic effect. Another point was that different group of

scientists used different cell type for cytotoxicity studies. Since different cells would have different response towards the same stimulus. It was suggested that it might be too early to say if MWCNT was cytotoxic or biocompatible unless more detail studies for each cell type has been done.

In MTT assay, significant difference was observed in samples cultured on different days. In day 2, significant difference was observed between PLLA and PLLA/MWCNT composite. We can see that the MD activity of PLLA/6.25% MWCNT and PLLA/5.00% composite had much higher than the control sample. It shows that the cells cultured on these composites have a higher metabolic rate than cell cultured on control sample. Similar observation was also found on day 4, 6 and 8. It suggested that PLLA/MWCNT composite might have certain properties outweigh the pure PLLA and unregulated the metabolic rate of HOB cell. In day 2 cell culture, PLLA sample with 5.00% and 6.25% had roughly two folds of MD activity than the control group. In day 4, PLLA with 6.25% MWCNT composite had approximately double of MD activity. In day 6 and day 8, PLLA with 3.75% MWCNT or more had approximately two folds of MD activity. It seems that the highest MD activity could be found from sample with 3.75% or more MWCNT. Most of the samples in these groups could double the MD activity. It was found that PLLA with 3.75% or more MWCNT could give the largest increase in MD activity.

According to the study done by Mei et al (2007), they cultured two different types of cell named gingival epithelial cells (GEC) and periodontal ligament cells (PLC) on electrospun PLLA/MWCNT membrane. From the MTT assay, the GEC cells gave lower MD activity than the control sample while PLC cells gave double MD activity result than the control sample on the third culture day. It seemed that the effect of

MWCNT to cell activity was cell type-dependent. Therefore, it further supported the controversy cytotoxicity result of MWCNT when culturing with different cells. Therefore, MWCNT can be a potential material for biomaterial reinforcement for HOB cell and PLC cell.

In ALP assay, PLLA samples with MWCNT had higher ALP enzyme activity than the control samples. It suggested that the addition of MWCNT, which increases the mechanical properties of the composite, could increase the differentiation marker of osteoblast-like cell. Statistically, no significant difference was observed for all sample cultured for 2, 4, 6 and 8 days. After two days culture, we could observe that the ALP activity is the highest for PLLA/5.00% MWCNT composite, which coincided with the cell metabolism assay. The control had the lowest ALP activity. At the forth day, the control had the lowest ALP activity again. PLLA/6.25% MWCNT composite had the highest ALP activity. At the sixth day, the activity of ALP of cell cultured on PLLA/5.00% composite was the highest. After eight days culture, cell cultured on PLLA/5.00% MWCNT composite has the highest ALP activity. It seems that PLLA sample with 3.75% or above MWCNT can give the most effective simulate to the activity of ALP enzyme. This may explained that the MTT activity is somehow related to the ALP activity. However, the PLLA/MWCNT composite might not give significant upregulating effect on the ALP activity, which represented the differentiation phenotype.

Even MWCNT cannot give significant upregulating of ALP activity as hydroxyapatite. MWCNT is a highly potential material for tissue engineering because it allows covalent functionalization by various components. In the past, functionalization of CNT is a challenging task because it was inherently unreactive and bundled (Martinez-Rubi et al., 2007). However, various attempts have been made and Martinez-

Rubi et al (2007) has discovered a convenient method for CNT functionalization at room temperature. Even though there is no functionalization of CNT with collagen, calcium complex and other bone related protein, to the best of my knowledge, the simplification of CNT processing would certainly raise interest of scientists to synthetic "bioactive CNT". Moreover, the excellent electrical conductivity enables the possibility to apply the electrical stimulation to the cell cultured on the composite. This is not possible for non-conducting PLLA/HA composite.

Chapter 6: Conclusion and future studies

6.1. Conclusion

PLLA/MWCNT composite has been fabricated successfully by solvent-casting method. From the result of nanoindentation, the mechanical properties of PLLA/MWCNT increases with the addition of MWCNT. MWCNT is an efficient material for reinforcement as 5% of MWCNT can doubles the Young's modulus of PLLA composite comparing with the control sample. It was found that MWCNT reinforcement is more efficient than HA reinforcement. XRD and EDX test has been carried out and confirm the successful integration of MWCNT into the PLLA.

Surface morphology was monitored by SEM and found some protruded MWCNT nanofibres; this protruded nanofibre may have adverse effect on cell adhesion. It is expected that this adverse effect can be overcome by the continuously increase of Young's modulus. Osteoblast-like cell was cultured on different PLLA/MWCNT. The cell had high viability and did not exhibit significant difference in viability between PLLA/MWCNT composite and control sample. No significant cytotoxic effect of PLLA/MWCNT was found. From the MD and ALP assay, we found that osteoblast-like cell had generally higher MD and ALP activity than the control. PLLA samples with 3.75% or more MWCNT generally gives higher MD and ALP activity than sample with MWCNT content below 2.5% and control sample. The increase in MD activity explained the increase in metabolic rate of cell. The ALP activity was involved in the bone-matrix deposit of osteoblast-like cell and the increase in ALP activity suggests that the composite can stimulate the bone-matrix deposit. However, there is no significant difference among ALP activity in each culture period. Even thought PLLA/MWCNT cannot activate the ALP activity of HOB cell significantly. Functionalization of

MWCNT is possible and can be a good solution to address this weakness. Therefore, PLLA/MWCNT can be an attractive candidate for scaffold fabrication for HOB cell culture.

6.2. Limitation

In this study, since the interaction of HOB cell and PLLA/MWCNT composite were carried out for eight days only, it was sufficient to evaluate the short-term effects of PLLA/MWCNT composites on cell only. Furthermore, PLLA/MWCNT composite was fabrication in form of thin film only and was cultured in vitro, it didn't mimic the complete in vivo environment and might affect the response of cell.

6.3. Future studies

In this study, the physical properties and biological performance of PLLA/MWCNT composite on osteoblast-like cell had been studied. However, there is several challenging area which is worth to explore further.

6.3.1. Fabrication of PLLA/MWCNT composite in other ratio

Since the mechanical properties are important to govern the response of osteoblast-like cell. More different ratio of PLLA and MWCNT composite can be fabricated to understand more about the changes in mechanical properties of PLLA/MWCNT under different ratio. Then cell study can be carried out to figure out the optimal ratio.

6.3.2. Long term degradation study of PLLA/MWCNT composite

PLLA is a biodegradable biomaterial. Because of its slow degradating properties, the study of relationship between degradation rate and mechanical properties of PLLA/MWCNT composite in long term are important as biodegradability govern the potential application in scaffold fabrication for bone tissue engineering. Even though PLLA/MWCNT is slow degradating and has low risk of MWCNT release in short term. It is still not clear if MWCNT has any adverse on cell in long term. Therefore, monitoring the potential release of MWCNT may be carried out in parallel during the degradation study.

6.3.3. Fabrication PLLA/MWCNT scaffold

In the real application, porous PLLA/MWCNT scaffold should also be fabricated in later stage to study the degradation rate and MWCNT release. Cell study should be carried out to evaluate the best pore size and porosity for tissue engineering.

6.3.4. Monitoring other cell-specific protein

Osteoblast-like cell can express different kind of bone production or suppression protein such as osteocalcin, osteopontin and type-1 collagen. They should be monitored to provide a more information about the effect of PLLA/MWCNT composite on cells.

6.3.5. Culturing of other cell-type and animal study

Besides the osteoblast-like cell, it would be another challenge to see if PLLA/MWCNT can support the growth of other cell type for other potential application, such as chondrocyte for cartilage engineering. In the later stage, animal study should be carried out to evaluate the performance and animal response towards the scaffold. This is an important step before clinical trials.

Reference

Agrawal CM, Ray RB (2001). Biodegradable polymeric scaffolds for musculoskeletal tissue engineering. J Biomed Mater Res. 55(2):141-50.

Altman G, Horan R, Martin I, Farhadi J, Stark P, Volloch V, Vunjak-novakovic G, Richmond J (2002). Cell differentiation by mechanical stress. FASEB J 16:270-2.

Basso N, Heersche JNM (2002). Characteristics of In Vitro Osteoblastic Cell Loading Models. Bone 30:347-51.

Bianco A, Hoebeke J, Godefroy S, Chaloin O, Pantarotto D, Briand JP, Muller S, Prato M, Partidos CD. Cationic Carbon Nanotubes Bind to CpG Oligodeoxynucleotides and Enhance Their Immunostimulatory Properties. J Am Chem Soc. 127(1):58-9.

Boland ED, Coleman BD, Barnes CP, Simpson DG, Wnek GE, Bowlin GL (2005). Electrospinning polydioxanone for biomedical applications. Acta Biomater 1(1):115–23

Burgess EA, Hollinger JO (1998). Options for engineering bone. In: Patrick Jr CW, Mikos AG, McIntire LV. Frontiers in tissue engineering. Pergamon Press. pp383-99.

Burr DB (2002). Targeted and nontargeted remodeling. Bone 30(1):2-4.

Burr DB, Milgrom C, Fyhrie D, Forwood MR, Nyska M, Finestone A, Hoshaw S, Saiag E, Simkin A (1996). In vivo measurement of human tibial strains during vigorous activity. Bone 18:405-10.

Cancedda R, Giannoni P, Mastrogiacomo M (2007). A tissue engineering approach to bone repair in large animal models and in clinical practice. Biomater 28(29):4240-50.

Chen GX, Kim HS, Park BH, Yoon JS (2005). Controlled Functionalization of Multiwalled Carbon Nanotubes with Various Molecular-Weight Poly(L-lactic acid). J Phys Chem B 109:22237-43.

Chen Y, Mak AFT, Li J, Wang M, Shum AWT (2005). Formation of paptite on poly(α-hydroxy acid) in an accelerated biominetic process. J Biomed Mater Res B Appl Biomater 73B:68-76.

Cherukuri P, Bachilo SM, Litovsky SH, Weisman RB (2004). Near-Infrared Fluorescence Microscopy of Single-Walled Carbon Nanotubes in Phagocytic Cells. J Am Chem Soc 126(48):15638-9.

Ciapetti G, Ambrosio L, Savarino L, Granchi D, Cenni E, Baldini N, Pagani S, Guizzardi S, Causa F, Giunti A (2003). Osteoblast growth and function in porous poly ε-caprolactone matrices for bone repair: a prelimary study. Biomater 24:3815-24.

Coombes AG, Heckman JD (1992A). Gel casting of resorbable polymers. 1. Processing and applications. Biomater 13:217-24.

Coombes AG, Heckman JD (1992B). Gel casting of resorbable polymers. 2. In vitro degradation of bone graft substitutes. Biomater 13:297-307.

Coombes AGA, Rizzi SC, Williamson M, Barralet JE, Downes S, Wallace WA (2004). Precipitation casting of polycaprolactone for applications in tissue engineering and drug delivery. Biomater 25(2):315-25

Crawford RW, Murray DW (1997). Total hip replacement: indications for surgery and risk factors for failure. Ann Rheum Dis 56:455–7

Cui D, Tian F, Schwarz H, Estrada GG, Kobayashi H.Cytotoxicity of single-wall carbon nanotubes on human fibroblasts. Toxicol In Vitro 20(7):1202-12.

Dalby MJ, Silvio LD, Harper EJ, Bonfield W (2001). Increasing hydroxyapatite incorporation into poly(methylmethacrylate) cement increases osteoblast adhesion and response. Biomaterials 23:569-76.

Gay CV (2005). The Osteoclast. In: Hollinger JO, Einhorn TA, Doll BA, Sfeir C, editors. Bone tissue Engineering, CRC Press. pp55-87.

Gazell Mapili, Yi Lu, Sahochen Chen, Krishnendu Roy (2005). Laser-Layered Microfabrication of Spatially Patterned Functionalized Tissue-Engineering Scaffolds. J Biomed Mater Res Part B: Appl Biomater 75B:414-24.

Giordano RA, Wu BM, Borland SW, Cima LG, Sachs EM, Cima MJ (1996). Mechanical properties of dense polylactic acid structures fabricated by three dimensional printing. J Biomater Sci Polym Ed 8:63-75.

Grunlan JC, Liu L, Regev O (2008). Weak polyelectrolyte control of carbon nanotube dispersion in water. J Colloid Interface Sci 317(1):346-9.

Harber K, Kuehn M, Delius H (1984). Insertion of retrovirus into the first intron of alpha1(I) collagen gene leads to embryonic lethal mutation in mice. Proc Matl Acad Sci USA 81:1504-8.

Harris LD, Kim BS, Mooney DJ (1998). Open pore biodegradable matrices formed with gas foaming. J Biomed Mater Res 42: 396-402.

Harrison BS, Atala A (2007). Carbon nanotube applications for tissue engineering. Biomater 28(2):344-53.

Hartig M, Joos U, Wiesmann H (2000). Capacitively coupled electric fields accelerate proliferation of osteoblast-like primary cells and increase bone extracellular matrix formation in vitro. Eur Biophys J 29:499-506.

Hill PA (1998). Bone Remodelling. British J Orthodontics 25:101-7

Hsu YY, Gresser JD, Trantolo DJ, Lyons CM, Gangadharam PR, Wise DL (1997). Effect of polymer foam morphology and density on kinetics of in vitro controlled release of isoniazid from compressed foam matrices. J Biomed Mater Res 35: 107-16.

Hull C (1990) Method for production of three-dimensional objects by stereolithography. US Patent 4929402

Iijima S (1991). Helical microtubules of graphitic carbon. Nature 354:56-8

Islam MF, Rojas E, Bergey DM, Johnson AT, Yodh AG (2003). High Weight Fraction Surfactant Solubilization of Single-Wall Carbon Nanotubes in Water. Nano Lett 3(2):269-73.

Jain RA, (2000) The manufacturing techniques of various drug loaded biodegradable poly(lactide-co-glycolide) (PLGA) devices. Biomater 21:2475-90.

Jia G, Wang H, Yan L, Wang X, Pei R, Yan T, Zhao Y, Guo X (2005). Cytotoxicity of carbon nanomaterials: single-wall nanotube, multi-wall nanotube and fullerene. Environ Sci Technol 39(5):1378-83

Juliano RL (2002). Signal Transduction by cell adhesion receptors and the cytoskeleton. Annu Rev Pharmacol Toxicol 42: 283-323.

Jung RE, Cochran DL, Domken O, Seibl R, Jones AA, Buser D, Hammerle CH (2007). The effect of matrix bound parathyroid hormone on bone regeneration. Clin Oral Implants Res 18(3):319-25.

Kadiyala S, Lo H, Leong KW (1994). Biodegradable Polymers as Synthetic Bone Grafts. In: Brighton CT, Friedlaender G, Lane JM, editors. Bone Formation and Repair. American Academy of Orthopaedic Surgeons. pp317-324.

Kapur S, Mohan S, Baylink DJ, Lau KH (2005). Musculoskeletal Disease Center, Jerry L. Pettis Memorial Veterans Fluid shear stress synergizes with insulin-like growth factor-I (IGF-I) on osteoblast proliferation through integrin-dependent activation of IGF-I mitogenic signaling pathway. J Biol Chem 280(20):20163-70.

Keegan GM, Learmonth ID, Case CP (2007). Orthopaedic metals and their potential toxicity in the arthroplasty patient: A review of current knowledge and future strategies. J Bone Joint Surg Br 89(5):567-73.

Kim CW, Talac R, Lu L, Moore MJ, Currier BL, Yaszemski MJ (2007). Characterization of porous injectable poly-(propylene fumarate)-based bone graft substitute. J Biomed Mater Res A (in print).

Landers R, Mulhaupt R (2000) Desktop manufacturing of complex objects, prototypes and biomedical scaffolds by means of computer-assisted design combined with computer-guided 3D plotting of polymers and reactive oligomers. Macromol Mater Eng 282:17-21.

Lee KW, Wang S, Lu L, Jabbari E, Currier BL, Yaszemski MJ (2006). Fabrication and Characterization of Poly(Propylene Fumarate) Scaffolds with Controlled Pore Structures Using 3-Dimensional Printing and Injection Molding. Tissue Eng 12(10):2801-11

Li D, Wang H, Zhu J, Wang X, Lu L, Yang X (2003). Dispersion of carbon nanotubes in aqueous solutions containing poly(diallyldimethylammonium chloride). J Mater Sci Letters 22:253–5

Li Q, Kinloch IA, Windle AH (2005). Discrete dispersion of single-walled carbon nanotubes. Chem Commun. 26:3283-5.

Liao SS, Cui FZ, Zhang W, Feng QL (2004). Hierarchically biomimetic bone scaffold materials: Nano-HA/collagen/PLA composite. J Biomed Mater Res B Appl Biomater 69B:158-65.

Lu Q, Moore JM, Huang G, Mount AS, Rao AM, Larcom LL, Ke PC. RNA Polymer Translocation with Single-Walled Carbon Nanotubes. Nano Lett 4(12):2473-7.

Marks SC, Odgren PR (2002). Structure and development of the skeleton. In: Bilezikian JP, Raisz LG, Rodan GR, editors. Principles of bone biology. Academic Press. pp3-15.

Marra KG (2005). Biodegradable polymers and microspheres in tissue engineering. In: Hollinger JO, Einhorn TA, Doll BA, Sfeir C, editors. Bone tissue Engineering, CRC Press. pp149-66.

Martina M., Subramanyam G., Weaver JC, Hutmacher DW., Morse DE., Valiyaveettil S (2005). Developing macroporous bicontinuous materials as scaffolds for tissue engineering. Biomater 26:5609-16

Martinez-Rubi Y, Guan J, Lin S, Scriver C, Sturgeon RE, Simard B (2007). Rapid and controllable covalent functionalization of single-walled carbon nanotubes at room temperature. Chem Commun (48):5146-8.

Maysinger D, Morinville A (1997). Drug delivery to the nervous system. Trends Biotechnol 15(10):410-8.

Mei F, Zhong J, Yang X, Ouyang X, Zhang S, Hu X, Ma Q, Lu J, Ryu S, Deng X (2007). Improved biological characteristics of poly(L-lactic acid) electrospun membrane by incorporation of multiwalled carbon nanotubes/hydroxyapatite nanoparticles. Biomacromolecules 8(12):3729-35.

Meyer U, Buchter A, Wiesmann HP, Joos U, Jones DB (2005). Basic Reactions of osteoblasts on structured material surfaces. Euro Cells Mater 9:39-49.

Mikos AG, Sarakinos G, Leite SM, Vacanti JP, Langer R (1993). Laminated three-dimensional biodegradable foams for use in tissue engineering. Biomater 14(5):323-30.

Mooney DJ, Baldwin DF, Suh NP, Vacanti JP, Langer R (1996). Novel approach to fabricate porous sponges of poly(D,L-lactic-co-glycolic acid) without the use of organic solvents. Biomater 17:1417-22.

Noble BS, Peet N, Stevens HY, Brabbs A, Mosley JR, Reilly GC, Reeve J, Skerry TM, Lanyon LE (2003). Mechanical loading: biphasic osteocyte survival and targeting of osteoclasts for bone destruction in rat cortical bone. Am J Physiol Cell Physiol 284:C934-43

Oliver WC, Pharr GM (2003). Measurement of hardness and elastic modulus by instrumented indentation. J Mater Res 18(1):3-20

Owen GRh, Meredith DO, ap Gwynn I, Richards RG (2005). Focal adhesion quantification – a new assay of material biocompatibility? : Review. Euro Cells and Mater 9:85-96.

Pantarotto D, Briand JP, Prato M, Bianco A (2004). Translocation of bioactive peptides across cell membranes by carbon nanotubes. Chem Commun 1:16-7.

Patrick CW Jr, Mikos AG, McIntire LV (1998). Prospectus of Tissue Engineering. In: Patrick Jr CW, Mikos AG, McIntire LV, editors. Frontiers in tissue engineering. Pergamon Press. pp3-11.

Pazzaglia UG, Andrini L, Duccci AD (1997). The effects of mechanical forces on bones and joints. J Bone Joint Surg 79B:1024-30.

Peled E, Boss J, Bejar J, Zinman C, Seliktar D (2007). A novel poly(ethylene glycol)-fibrinogen hydrogel for tibial segmental defect repair in a rat model. J Biomed Mater Res A 80(4):874-84.

Peter SJ, Yaszemski MJ, Suggs LJ, Payne RG, Langer R, Hayes WC, Unroe MR, Alemany LB, Engel PS, Mikos AG (1997). Characterization of partially saturated poly(propylene fumarate) for orthopaedic application. J Biomater Sci Polym Ed 8:893-904.

Pitt CG, Jeffcoat AR, Zweidinger RA, Schindler A (1979). Sustained drug delivery systems. The permeability of poly(-caprolactone), poly(DL-lactic acid) and their copolymers. J Biomed Mat Res 13(12):497–507

Prigodich RV, Vesely MR (1997). Characterization of the complex between bovine osteocalcin and type 1 collagen. Arch Biochem Biophys 345:339-41.

Rai B, Teoh SH, Ho KH, Hutmacher DW, Cao T, Chen F, Yacob K (2004). The effect of rhBMP-2 on canine osteoblasts seeded onto 3D bioactive polycaprolactone scaffolds. Biomaterials 25:5499-506.

Rajdip B, Einat NR, Oren R, Rachel (2002). Stabilization of Individual Carbon Nanotubes in Aqueous Solutions. Nano Lett 2:25-8

Reinstorf A, Ruhnow M, Gelinsky M, Pompe W (2004). Phosphoserine – a convenient compoundd for modification of calcium phosphate bone cement collagen composites. J Mater Sci Mater Med 15:451-5.

Rizzi SC, Heath DJ, Coombes AGA, Bock N, Textor M, Downes S (2000). Biodegradable polymer/hydroxyapatite composites: surface analysis and initial attachment of human osteoblasts. J Biomed Mater Res 55:475-86.

Robey PG (1994). Normal Bone Formation and Structure. In: Brighton CT, Friedlaender G, Lane JM, editors. Bone Formation and Repair. American Academy of Orthopaedic Surgeons. pp3-12.

Sachlos E, Czernuszka JT (2003). Making tissue engineering scaffolds work. Review: the application of solid freeform fabrication technology to the production of tissue engineering scaffolds. Eur Cell Mater 5:29-39.

Schmitz JP, Hollinger JO (1988). A preliminary study of the osteogenic potential of a biodegradable alloplastic-osteoinductive alloimplant. Clin Orthop 237:245-55.

Schneider A, Francius G, Obeid R, Schwinte P, Hemmerle J, Frisch B, Schaaf P, Voegel J, Senger B, Picart C (2006). Polyelectrolyte Multilayers with a tunable young's modulus: influence of film stiffness on cell adhesion. Langmuir 22:1193-200.

Scott CS (1991) Apparatus and method for creating three-dimensional objects. US Patent 5121329.

Shah AK, Sinha RK, Hickok NJ, Tuan RS (1999). High-resolution morphometric analysis of human osteoblastic cell adhesion on clinically relevant orthopaedic alloys. Bone 24:499-506.

Shi G, Cai Q, Wang C, Lu N, Wang S, Bei J (2002). Fabrication and biocompatibility of cell scaffolds of poly(L-lactic acid) and poly(L-lactic-co-glycolic acid).Polymers for Advanced Technologies 13:227-32.

Shintaroh Iwanaga, Yoshikatsu Akiyama, Akihiko Kikuchi, Masayuki Yamato, Kiyotaka Sakai, Teruo Okano (2005). Fabrication of a cell array on ltrathin hydrophilic polymer gels utilising electron beam irradiation and UV excimer laser ablation. Biomater 26:5395-404.

Shvedova AA, Castranova V, Kisin ER, Schwegler-Berry D, Murray AR, Gandelsman VZ, Maynard A, Baron P (2003). Exposure to carbon nanotube material: assessment of nanotube cytotoxicity using human keratinocyte cells. J Toxicol Environ Health A 66(20):1909-26.

Sikavitsas VI, Temenoff JS, Mikos AG. (2001). Biomaterials and bone mechanotransduction. Biomaterials 22:2581-93.

Singhal AR, Agrawal CM, Athanasiou KA (1996). Salient degradation features of a 50:50 PLA/PGA scaffold for tissue engineering. Tissue Eng 2:197-207.

Tan L, Kong YP, Bao LR, Huang XD, Guo LJ, Pang SW, Yee AF (2003). Imprinting polymer film on patterned substrates. J Vac Sci Technol B 21:2742-8.

Taylor D, Hazenberg JG, Lee TC (2003), The cellular transducer in damage-stimulated bone remodelling: a theoretical investigation using fracture mechanics. J of Theoretical Biology 225:65-75.

Thanki PN, Dellacherie E, Six JL (2006). Surface characteristics of PLA and PLGA films. Appl Surf Sci 253:2758-64.

Verhaar JA. (2007). Prognosis of total hip replacement: the importance of an implant register. Ned Tijdschr Geneeskd. 151(35):1915-7.

Westbroek I, Ajubi NE, Alblas MJ, Semeins CM, Klein-Nulend J, Burger EH, Nijweide PJ (2000). Differential Stimulation of Prostaglandin GH Synthase-2 in Osteocytes and Other Osteogenic Cells by Pulsating Fluid Flow. Biochem Biophys Res Comm 268:414-9.

Wiesmann HP, Klatt C, Szuwart T, Meyer U (2003). Bone tissue engineering by primary osteoblast-like cells in a monolayer system and 3-dimensional collagen gel. J Oral Maxillofac Surg 61:1455-62.

Wright-Charlesworth DD, King JA, Miller DM, Lim CH (2006). In vitro flexural properties of hydroxyapatite and self-reinforced poly(L-lactic acid). J Biomed Mater Res A 78(3):541-9.

Xin AX, Gaydos C, Mao JJ (2006). In vitro Degradation Behavior of Photopolymerized PEG Hydrogels as Tissue Engineering Scaffold. Conf Proc IEEE Eng Med Biol Soc 1:2091-3.

Yamaguchi M, Shinbo T, Kanamori T, Wang P, Niwa Motohiro, Kawakami H, Nagaoka S, Hirakawa K, Kamiya M (2004). J Artif Organ 7:187-93.

Yang DQ, Jean-Francois Rochette, Edward Sacher (2005). Functionalization of Multiwalled Carbon Nanotubes by Mild Aqueous Sonication. J Phys Chem B 109(16):7788-94.

Yang Y, Basu S, Tomasko DL, Lee LJ, Yang ST (2004). Fabrication of well-defined PLGA scaffolds using novel microembossing and carbon dioxide bonding. Biomater 26:2585-94

Yang Y, Basu S, Tomasko DL, Lee LJ, Yang ST (2005). Fabrication of well-defined PLGA scaffolds using novel microembossing and carbon dioxide bonding. Biomater 26(15):2585-94.

You J, Yellowley CE, Donahue HJ, Zhang Y, Chen Q, Jacobs CR (2000). Substrate Deformation Levels associated with Routine physical activity are less stimulatory to bone cells relative to loading-induced oscillatory fluid flow. J Biomech Eng 122:387-93.

Yuan X, Mak AFT, Li J (2001). Formation of bone-like apatite on poly(L-lactic acid) fibers by a biomimetic process. J Biomed Mater Res 57:140-50.

Zhang D, Kandadai MA, Cech J, Roth S, Curran SA (2006). Poly(L-lactide) (PLLA)/Multiwalled Carbon Nanotube (MWCNT) Composite: Characterization and Biocompatibility Evaluation. J Phys Chem B 110:12910-5.